Quantum system dynamics with a weakly nonlinear Josephson junction bath

Jing Yang [1], Étienne Jussiau [1], Cyril Elouard [1], Karyn Le Hur,[2] and Andrew N. Jordan [1,3]
[1]*Department of Physics and Astronomy, University of Rochester, Rochester, New York 14627, USA*
[2]*CPHT, CNRS, Institut Polytechnique de Paris, Route de Saclay, 91128 Palaiseau, France*
[3]*Institute for Quantum Studies, Chapman University, 1 University Drive, Orange, California 92866, USA*

(Received 20 August 2020; revised 11 December 2020; accepted 6 January 2021; published 1 February 2021)

We investigate the influence of a weakly nonlinear Josephson bath consisting of a chain of Josephson junctions on the dynamics of a small quantum system (LC oscillator). Focusing on the regime where the charging energy is the largest energy scale, we perturbatively calculate the correlation function of the Josephson bath to the leading order in the Josephson energy divided by the charging energy while keeping the cosine potential exactly. When the variation of the charging energy along the chain ensures fast decay of the bath correlation function, the dynamics of the LC oscillator that is weakly and capacitively coupled to the Josephson bath can be solved through the Markovian master equation. We establish a duality relation for the Josephson bath between the regimes of large charging and Josephson energies, respectively. The results can be applied to cases where the charging energy either is nonuniformly engineered or disordered in the chain. Furthermore, we find that the Josephson bath may become non-Markovian when the temperature is increased beyond the zero-temperature limit in that the bath correlation function gets shifted by a constant and does not decay with time.

DOI: 10.1103/PhysRevB.103.085402

I. INTRODUCTION

Realistic quantum systems are inevitably interacting with their surrounding environment, which induces decoherence and dissipation. In these situations, one is usually only interested in the dynamics of the primary system. Therefore some procedure that traces out the environmental degrees of freedom is required. In the past years, numerous approaches have been developed to reach this goal, including the Markovian equation developed by Gorini–Kossakowski–Sudarshan and Lindblad independently [1–4], stochastic Schrödinger equations [5–9], the quantum Langevin equation [10], the Feynman–Vernon influence functional techniques [11–15], nonequilibrium Green's functions initiated by Schwinger [16], further developed by Keldysh [17] and Kadanoff–Baym [18]. For a recent overview of the various approaches, see the review article by de Vega and Alonso [19].

These sophisticated techniques, on which most of previous works have focused typically, assume either a harmonic bath (see the discussion in Breuer and Petruccione's well-known textbook [4]) or an anharmonic bath whose baseline is harmonic [20,21]. Situations where a harmonic bath is coupled to a nonlinear quantum system have been widely studied within this framework. It has been shown that coupling to a nonlinear degree of freedom in the small quantum system enabled to probe many-body effects. The advent of circuit QED [22] has given rise to recent experimental efforts in this direction [23–39]. Typically, the nonlinear small quantum system can be either represented by a two-level quantum system [13,14,23,24,27–30,33–36,39], which characterizes the low-energy effective physics of a particle tunneling into a double-well potential or a Josephson junction [23,25,26,37,38], which is a naturally present source of nonlinearity in circuit-QED based qubits. This type of system has been studied extensively, ranging from the weak coupling regime [23], where the junction parameters obtain a small renormalization, to the strong coupling regime [24,26,27,30,33–42], where an appreciable Lamb shift is produced.

Conversely, the influence of an anharmonic environment on a small quantum system has seldom been investigated. However, the experimental study of open quantum systems with exotic properties, beyond the usual assumption of a harmonic bath, is nowadays possible owing to advances in quantum bath engineering [43]. There are previously works focuing on spin bath, summarized in the review article [44]. Here, we investigate another type of nonharmonic bath, which consisiting of an array of Josephson junctions. Motivated by further technological progress [45], we analyze in this article the dynamics of quantum system coupled to a weakly nonlinear one-dimensional Josephson junction array (JJA). The regime where the Josephson energy is the largest energy scale in play can be treated within the harmonic approximation, and the JJA then behaves as a set of harmonic oscillators to leading order. The next-to-leading-order nonlinear behavior can be well-characterized by the $\lambda\varphi^4$ type of nonlinearity in the usual language of anharmonic oscillators [25,32,46,47], and the Kerr effect associated to such a nonlinearity has already been analyzed [32]. (Here φ denotes the Josephson junction phase difference, one of the two quadratures of the oscillators with the charge difference.) In this work, we will be focusing on the opposite limit where the charging energy is much larger the Josephson energy and the temperature so that the full

nonlinearity of the cosine Josephson potential must be taken into account.

Although the strong-coupling regime brings along interesting physics, we will consider here that the JJA is weakly coupled to the quantum system as a first step to probe the nonlinear environment. We compute the JJA bath correlation function to leading order in the regime of large charging energy using time-independent degenerate perturbation theory. We show that, when the nonlinear term is present and the distribution of the Josephson junction parameters is properly engineered or presents sufficient disorder, the JJA correlation function decays rapidly so that the chain behaves as a Markovian bath. The Markovianity of the JJA bath provides a route to find the dynamics of the primary quantum system within the framework of the Gorini–Kossakowski–Sudarshan–Lindblad (GKSL) master equation. To leading order, we find that the JJA bath correlation function mimics that of a harmonic bath at zero temperature, with an effective spectral density which depends on the distribution of the various junction parameters. Since the harmonic bath can be emulated by the leading order approximation of the JJA bath in the large Josephson energy regime, we establish a duality relation for the JJA in the large charging energy and the large Josephson energy regimes, which yields exactly the same coarse-grained dynamics for the small system. However, when temperature is increased beyond the zero temperature limit, we show that the dynamics of the small system becomes non-Markovian as the JJA correlation function acquires a time-independent shift that we connect to the physics of the free rotors, modeling the leading-order behavior of the JJA.

This paper is organized as follows: In Sec. II, we derive the Hamiltonian of the JJA weakly coupled to an LC circuit from the standard procedure of circuit quantization. In Sec. III, we compute the correlation function of the JJA in the large charging energy regime from time-independent perturbation theory. This result can also be derived using the Matsubara formalism as detailed in Appendix B 2. In Sec. IV, we discuss the temperature driven non-Markovian effects. In Sec. V, we compute the Lamb shift and decay rate of the damped LC oscillator within the GKSL master equation framework using the correlation function obtained in Sec. III. Furthermore, we also discuss the bath duality relation between the large charging energy and large Josephson energy regimes in the zero-temperature limit. We give three specific examples in Sec. VI. We summarize our findings and discuss future directions in Sec. VII.

II. THE MODEL AND ITS PHYSICAL IMPLEMENTATION

A. General description of the model

Throughout this paper, we shall set $\hbar = k_B = 1$. The Hamiltonian of the JJA, which we will derive from first principles shortly, is

$$H_B = \sum_\alpha E_{C\alpha} N_\alpha^2 - \sum_\alpha E_{J\alpha} \cos\varphi_\alpha, \tag{1}$$

where $E_{C\alpha} \equiv 2e^2/C_\alpha$ and $E_{J\alpha}$, respectively, are the charging and Josephson energy for junction α, while φ_α and N_α are canonically conjugated variables, i.e.,

$$[\varphi_\alpha, N_\beta] = i\delta_{\alpha\beta}. \tag{2}$$

The JJA is capacitively coupled to the quantum system of interest. The system Hamiltonian is denoted by H_S, while the coupling Hamiltonian is written as

$$H_I = S \sum_\alpha g_\alpha N_\alpha. \tag{3}$$

In principle, the system Hamiltonian H_S and the system coupling operator S can be chosen arbitrarily. We will now show that when the system is an LC circuit capacitively coupled to the JJA as shown in Fig. 1(a), then the Hamiltonian of the system and interaction terms are

$$H_S = \frac{Q^2}{2C} + \frac{\Phi^2}{2\mathcal{L}}, \tag{4}$$

$$H_I = Q \sum_{\alpha=1}^{N_J} g_\alpha N_\alpha. \tag{5}$$

Here C is the capacitance of the LC oscillator which is renormalized due to the coupling to the JJA, $\mathcal{L}$ is the inductance of the LC oscillator and N_J is the number of junctions in the JJA, while the operators Q and Φ correspond to the charge of the capacitor and the magnetic flux of the inductor, respectively. These operators are canonically conjugated,

$$[\Phi, Q] = i. \tag{6}$$

B. Derivation of the Hamiltonian

With the quantization procedure for mesoscopic circuits reviewed by Devoret [50], one can write the Lagrangian L_{tot} of the circuit in Fig. 1(a) as follows:

$$L_{tot} = \frac{1}{2}\sum_{\alpha=1}^{N_J} C_\alpha \Phi_0^2 (\dot\theta_\alpha - \dot\theta_{\alpha+1})^2 + \sum_{\alpha=1}^{N_J} E_{J\alpha}\cos(\theta_\alpha - \theta_{\alpha+1}) + \frac{1}{2}C_I(\Phi_0\dot\theta_1 - \dot\Phi)^2 + \frac{1}{2}C\dot\Phi^2 - \frac{1}{2\mathcal{L}}\Phi^2, \tag{7}$$

where θ_α is the phase at the superconducting island α and we set the ground at the extremity of the chain such that $\theta_{N_J+1} = 0$ and $\Phi_0 = 1/(2e)$ is the magnetic flux quantum. The charge operator $\tilde N_\alpha$ canonically conjugated to the phase operator θ_α is for $\alpha = 1$,

$$2e\tilde N_1 \equiv \frac{1}{\Phi_0}\frac{\partial L_{tot}}{\partial\dot\theta_1} = C_1\Phi_0(\dot\theta_1 - \dot\theta_2) + C_I(\Phi_0\dot\theta_1 - \dot\Phi), \tag{8}$$

and for $\alpha > 1$,

$$2e\tilde N_\alpha \equiv \frac{1}{\Phi_0}\frac{\partial L_{tot}}{\partial\dot\theta_\alpha} = C_{\alpha-1}\Phi_0(\dot\theta_\alpha - \dot\theta_{\alpha-1}) + C_\alpha\Phi_0(\dot\theta_\alpha - \dot\theta_{\alpha+1}). \tag{9}$$

Upon making the following change of variables,

$$\varphi_\alpha = \theta_\alpha - \theta_{\alpha+1}, \tag{10}$$

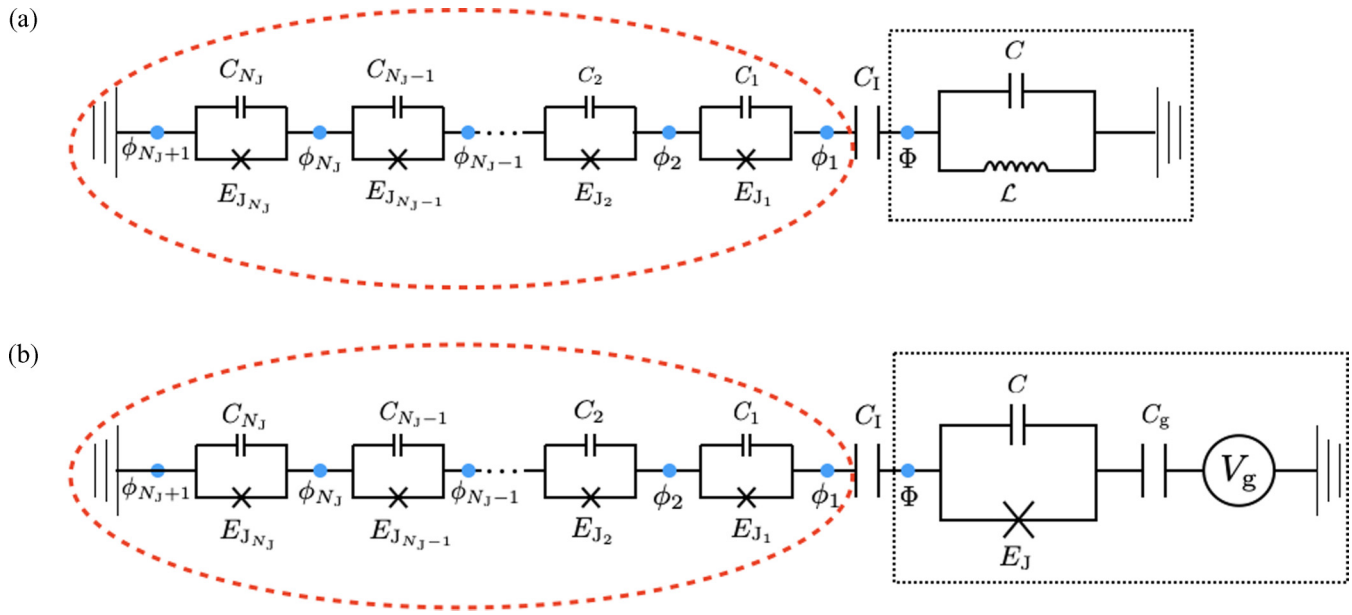

FIG. 1. (a) An LC oscillator in the right-hand side and (b) a single Cooper-pair box in the right-hand side weakly coupled to a one-dimensional JJA in the left-hand side of both figures. The charging and Josephson energies are assumed to vary across the chain in such a way that the JJA bath correlation function decays rapidly. Here, the stray capacitances between the islands and the ground are neglected, different from the extensively studied geometry of JJA in the literature [48,49], where the capacitances between neighboring islands are neglected but the stray capacitances are kept nonzero.

the degrees of freedom for the JJA in the total Lagrangian in Eq. (7) become noninteracting, i.e.,

$$L_{\rm tot} = \frac{1}{2}\sum_{\alpha=1}^{N_J} C_\alpha \Phi_0^2 \dot{\varphi}_\alpha^2 + \sum_{\alpha=1}^{N_J} E_{J\alpha}\cos\varphi_\alpha + \frac{1}{2}C_I(\Phi_0\sum_{\alpha=1}^{N_J}\dot{\varphi}_\alpha - \dot{\Phi})^2 + \frac{1}{2}C\dot{\Phi}^2 - \frac{1}{2\mathcal{L}}\Phi^2, \quad (11)$$

where we have used the fact that $\theta_1 = \sum_{\alpha=1}^{N_J}\varphi_\alpha$. The charge operator canonically conjugated to the phase operator φ_α is

$$2eN_\alpha \equiv \frac{1}{\Phi_0}\frac{\partial L_{\rm tot}}{\partial\dot{\varphi}_\alpha} = C_\alpha\Phi_0\dot{\varphi}_\alpha + C_I\left(\Phi_0\sum_{\alpha=1}^{N_J}\dot{\varphi}_\alpha - \dot{\Phi}\right). \quad (12)$$

According to Eqs. (8), (9), and (12), the charge operators $\tilde{N}_\alpha$ and N_α are related to each other through the following relation:

$$N_\alpha = \sum_{\beta=1}^{\alpha}\tilde{N}_\beta. \quad (13)$$

Clearly from this equation, N_α is a nonlocal charge operator, i.e., the sum of all the charge operators from the preceding islands. It is for this reason we shall call N_α and φ_α nonlocal variables and $\tilde{N}_\alpha$ and θ_α local variables. To gain some intuition about Eq. (13), we can relate the eigenstates of N_α to $\tilde{N}_\alpha$. It is clear that the eigenstate of the nonlocal charge operators $\{N_\alpha\}$, $|n_1, n_2, \cdots, n_{N_J}\rangle$ corresponds to the local charge state $|n_1, n_2-n_1, \cdots, n_{N_J}-n_{N_J-1}\rangle_{\rm loc}$, which is an eigenstate of the local charge operators $\{\tilde{N}_\alpha\}$. Therefore, we observe that a nonlocal charge excitation corresponds to a pair of local charge excitations with charge quantum number $+1$ and -1, respectively. In what follows, we shall work with the nonlocal operators instead of the local ones since it will simplify the calculation dramatically.

Hereafter, we will focus on the weak-coupling regime, corresponding to situations situations where C_I is small. In such cases, it is natural to assume that the bath degrees of freedom are only negligibly affected by the coupling to the LC oscillator. This assumption is in the same spirit as the celebrated Born approximation, widely used in the context of open quantum systems, which we apply to this setup in Sec. V. Therefore, the second term in the last equation of Eq. (12), due to the coupling to the LC oscillator, is ignored, which yields

$$2eN_\alpha \approx C_\alpha\Phi_0\dot{\varphi}_\alpha. \quad (14)$$

As regards the dynamics of the LC oscillator, we find

$$Q \equiv \frac{\partial L_{\rm tot}}{\partial\dot{\Phi}} = (C+C_I)\dot{\Phi} - C_I\Phi_0\sum_{\alpha=1}^{N_J}\dot{\varphi}_\alpha. \quad (15)$$

Then, we straightforwardly obtain

$$H_{\rm tot} = 2e\sum_{\alpha=1}^{N_J}N_\alpha\Phi_0\dot{\varphi}_\alpha + Q\dot{\Phi} - L_{\rm tot} = H_B + H_I + H_S, \quad (16)$$

where H_B, H_I, and H_S are defined in Eqs. (1), (3), and (4), respectively, and

$$C = C + C_I, \quad (17)$$

$$g_\alpha = \frac{2eC_I}{CC_\alpha} = \frac{\varepsilon_I E_{C\alpha}}{e}, \quad (18)$$

where $\varepsilon_I \equiv C_I/C$ characterizes the coupling strength of the LC oscillator to the JJA.

According to Eq. (14), $Q_\alpha \Phi_0 = N_\alpha$ and φ_α are canonically conjugated variables and therefore will satisfy Eq. (2) after being promoted to operators. Similarly, Eq. (6) follows from Eq. (15).

When the system is a qubit implemented by a Cooper pair box, as shown in Fig. 1(b), one can show going through a similar procedure that $H_S = \epsilon\sigma_x/2 + \omega_0\sigma_z/2$ and $H_I = \sigma_z \sum_\alpha g_\alpha N_\alpha$. In the Cooper pair box, σ_z represents the two-charge states close to a degeneracy point, ω_0 is controlled by V_g and measures deviations from the resonance for the two charge states, and ϵ is related to the Josephson energy E_J in Fig. 1(b). In what follows, we shall focus on the case where the system is an LC oscillator, as shown in Fig. 1(a)—except when it comes to the derivation of the JJA bath correlation function where the details of the primary system do not come into play.

In the LC circuit case, using the canonical commutation relation in Eq. (6), one can define the creation and annihilation operators

$$b^\dagger = \sqrt{\frac{C\omega_0}{2}}\left(\Phi - \frac{iQ}{C\omega_0}\right), \tag{19}$$

$$b = \sqrt{\frac{C\omega_0}{2}}\left(\Phi + \frac{iQ}{C\omega_0}\right), \tag{20}$$

where

$$\omega_0 \equiv 1/\sqrt{\mathcal{L}C} \tag{21}$$

refers to the plasma frequency in the LC system. Hence, Eqs. (4) and (5) become

$$H_S = \omega_0\left(b^\dagger b + \frac{1}{2}\right), \tag{22}$$

$$H_I = -i\sqrt{\frac{C\omega_0}{2}}(b - b^\dagger)\sum_\alpha g_\alpha N_\alpha. \tag{23}$$

III. CORRELATION FUNCTION OF THE JJA BATH

A. The central role of the bath correlation function

It is widely known that the dynamics of a "small" quantum system (an LC oscillator here) coupled to a large bath (the Josephson junction chain here) can be resolved thanks to the celebrated GKSL master equation [1–4], which has been proven to yield the most general Markovian evolution preserving the fundamental properties of the system density matrix. This formalism can be applied to a wide variety of situations, provided specific conditions are met by the system-bath coupling. Namely, to ensure that the master equation is Markovian, it is usually hypothesized that the coupling to the primary system negligibly influences the bath dynamics, which is typically the case when they are weakly coupled. In this context, the total system-bath density matrix is assumed to be factorized at all times, $\rho(t) = \rho_S(t) \otimes \rho_B$, where the (constant) bath density matrix ρ_B corresponds to the canonical distribution with inverse temperature β,

$$\rho_B = \frac{e^{-\beta H_B}}{\mathrm{Tr} e^{-\beta H_B}}. \tag{24}$$

While the interaction between the system and the bath induces correlations between the system and the bath, the evolution of such ansatz is a good approximation of the system dynamics coarse-grained over a timescale much larger than the correlation time of the bath, i.e., the timescale over which the correlations between the system and the bath decay [3]. This coarse-graining time must also be smaller than the typical decay time for the system, which is only possible if the correlation time is much smaller than this decay time. This coarse-grained dynamics is captured by the GKSL master equation. The existence of a finite, and small, correlation time for the bath can be verified by considering the appropriate correlation function of the bath, a central quantity for the study of Markovian open quantum systems. The choice of the relevant bath correlation function to analyze is dictated by the reservoir observable involved in the coupling Hamiltonian, which is the nonlocal charge operator N_α here. A brief derivation of the GKSL master equation highlighting the importance of the reservoir correlation function is given in Appendix A and the GKSL master equation is given by Eq. (79) with the coefficients given by Eqs. (80), (81) and (82) .

Furthermore, the GKSL formalism can only be used in situations where the coupling Hamiltonian satisfies [51]

$$\mathrm{Tr}_B[\rho_B H_I] = 0, \tag{25}$$

where the trace is taken over the bath degrees of freedom only. As such, since the coupling Hamiltonian H_I acts on both the system and bath, the right-hand side of Eq. (25) has to be understood as an operator acting on the system Hilbert space. When studying an LC oscillator coupled to a JJA, the coupling Hamiltonian is given in Eq. (5), which yields

$$\mathrm{Tr}_B[\rho_B H_I] = Q\sum_\alpha g_\alpha \langle N_\alpha\rangle . \tag{26}$$

Here $\langle\bullet\rangle$ denotes the average over the thermal state ρ_B in Eq. (24).

It turns out that the expectation value $\langle N_\alpha\rangle$ vanishes as a consequence of charge conjugation symmetry. This property concerns single junctions so we can temporarily drop the subscript α. Let us define the charge conjugation operator $\mathscr{C}$ such that $\mathscr{C}|n\rangle = |-n\rangle$. $\mathscr{C}$ is unitary and Hermitian: $\mathscr{C}^\dagger = \mathscr{C}^{-1} = \mathscr{C}$. It is straightforward to check that the number operator is odd under charge conjugation: $\mathscr{C}N\mathscr{C} = -N$. However, because of the commutation relation $[\varphi, N] = i$, one can easily show that $e^{\pm i\varphi}|n\rangle = |n \mp 1\rangle$ and therefore $\mathscr{C}(\cos\varphi)\mathscr{C} = \cos\varphi$. So we conclude that the junction Hamiltonian $H = E_C N^2 - E_J\cos\varphi$ is invariant under this transformation: $\mathscr{C}H\mathscr{C} = H$. We then have

$$\langle N\rangle = \frac{1}{Z}\mathrm{Tr}(e^{-\beta H}N) = \frac{1}{Z}\mathrm{Tr}(\mathscr{C}e^{-\beta H}\mathscr{C}\mathscr{C}N\mathscr{C}) = -\langle N\rangle . \tag{27}$$

It is then clear that $\langle N\rangle = 0$, which proves that Eq. (25) is satisfied here. The GKSL formalism can then be applied and the relevant correlation function for the JJA bath is given by

$$\Gamma(t) = \sum_\alpha g_\alpha^2 G_\alpha(t), \tag{28}$$

where $G_\alpha(t)$ is the correlation function for a single Josephson junction,

$$G_\alpha(t) = \langle N_\alpha(t)N_\alpha(0)\rangle . \tag{29}$$

Hereafter time-dependent operators indicate the interaction picture (Heisenberg picture with respect to Hamiltonian $H_{\rm B}$).

B. The large Josephson energy limit: The harmonic approximation

In what follows, we shall detail the calculation of the single-junction correlation function $G_\alpha(t)$ and then take the continuum limit to obtain the bath correlation function $\Gamma(t)$. The main aim of this paper is to discuss the large charging energy regime. However, before we head toward this end, let us first detour to discuss the extensively studied large Josephson energy regime, that is $E_{\rm C\alpha} \ll E_{\rm J\alpha}$ and $\beta^{-1} \ll E_{\rm J\alpha}$, where the harmonic bath approximation can be applied. [25,32] In this regime, thermal excitations are near a fixed minimum of the cosine potential and the effect of quantum phase slips may be neglected to leading order. In this case, the JJA bath can be approximated by a harmonic bath such that the bath Hamiltonian in Eq. (1) becomes

$$H_{\rm B} = \sum_\alpha \left[\frac{1}{2L_\alpha}\Phi_\alpha^2 + \frac{1}{2}L_\alpha \omega_\alpha^2 Q_\alpha^2 \right], \tag{30}$$

where $L_\alpha = \Phi_0^2/E_{\rm J\alpha}$ is the effective Josephson inductance—not to be confused with the total Lagrangian $L_{\rm tot}$—and ω_α is the characteristic frequency of the oscillator given by

$$\omega_\alpha = \frac{1}{\sqrt{L_\alpha C_\alpha}} = \sqrt{2E_{\rm J\alpha}E_{\rm C\alpha}}. \tag{31}$$

Even though $E_{\rm C\alpha} \ll E_{\rm J\alpha}$, the characteristic frequency ω_α can still take values in a wide spectrum. Therefore, by properly controlling the variations of the charging and Josephson energies along the JJA, one can still emulate a harmonic bath, which is usually implemented in transmission lines. The correlation function for a harmonic oscillator is well-known [4], namely,

$$G_\alpha(t) = \frac{\omega_\alpha}{4E_{\rm C\alpha}}\left[\coth\left(\frac{\beta\omega_\alpha}{2}\right)\cos(\omega_\alpha t) - i\sin(\omega_\alpha t)\right]. \tag{32}$$

Since a genuine thermal bath has infinitely many degrees of freedoms, we have to find the correlation function in the continuum limit. To this end, we assume that Josephson junctions are spatially distributed along the JJA according to the density $\nu(x)$. The JJA correlation function is then given by

$$\Gamma(t) = \int dx \nu(x) g^2(x) G(x,t), \tag{33}$$

where the junction number index α has been replaced by the position variable x, and the explicit expression for the coupling parameter $g(x)$ is analogous to that given in Eq. (18). Through a simple change of variables, it is straightforward to obtain

$$\Gamma(t) = \left(\frac{\varepsilon_{\rm I}}{2e}\right)^2 \int d\omega J(\omega)\left[\coth\left(\frac{\beta\omega}{2}\right)\cos(\omega t) - i\sin(\omega t)\right], \tag{34}$$

where $J(\omega)$ is the spectral density defined as

$$J(\omega) = \sum_k \omega \nu_k(\omega) E_{\rm C}^{(k)}(\omega)\left|\frac{dx_k}{d\omega}(\omega)\right|. \tag{35}$$

Here the index k labels the different intervals I_k on which $\omega(x)$ is a monotonic function. On each of these intervals, $\omega(x)$ can be inverted and $x_k(\omega)$ denotes the corresponding inverse function. From this, we define

$$\nu_k(\omega) \equiv \nu[x_k(\omega)], \tag{36}$$

$$E_{\rm C}^{(k)}(\omega) \equiv E_{\rm C}[x_k(\omega)]. \tag{37}$$

Hereafter, we will focus on the low-temperature regime where $\beta^{-1} \ll \omega(x)$ for (almost) all x. In that case, Eq. (34) becomes

$$\Gamma(t) = \left(\frac{\varepsilon_{\rm I}}{2e}\right)^2 \int_0^\infty d\omega J(\omega) e^{-i\omega t}. \tag{38}$$

It should be noted that in the large $E_{\rm J}$ regime where $E_{\rm C}(x) \ll E_{\rm J}(x)$, the condition $\beta^{-1} \ll \omega(x)$ implies that $\beta^{-1} \ll E_{\rm J}(x)$.

For the extensively studied geometry of JJA, where the stray capacitances are nonvanishing but the capacitances between neighboring islands are neglected [48,49], in large Josephson energy and zero-temperature limits, one can show that $\Gamma(t)$ decays as power-law according to Eq. (38), due to the linear dispersion relation of sound modes characterizing the lead-order effects of the JJA. However, in our setup shown in Fig. 1, the behavior of $\Gamma(t)$ is controlled by the distribution of the junction parameters in real space, rather than the sound modes in the momentum space. Therefore, in our setup $\Gamma(t)$ does not necessarily decay as power law in large Josephson energy and zero-temperature limits.

C. The large charging energy limit

In the remainder of this article, we focus on the large charging energy limit, where

$$E_{\rm J\alpha} \ll E_{\rm C\alpha},\ \sqrt{E_{\rm C\alpha}\delta E_{\rm C}}, \tag{39}$$

$$\beta^{-1} \ll \Delta_\alpha \equiv \frac{E_{\rm C\alpha}}{-\ln\lambda_\alpha}, \tag{40}$$

where $\lambda_\alpha \equiv E_{\rm J\alpha}/E_{\rm C\alpha} \ll 1$ and $\delta E_{\rm C}$ is the width of the effective spectral density of the Josephson bath [defined subsequently in Eq. (75)], which represents the characteristic frequency of the bath. In this regime, the physics is dominated by capacitors, which are quantum mechanically equivalent to free rotors from Eq. (1). The ground state fixes the charge but the phase variable can fluctuate accordingly. Thermal excitation in a junction is negligible so that each junction stays in the exact ground state of the total Hamiltonian to the leading order. Based on this intuition, we can evaluate $G_\alpha(t)$ to second order in λ_α at low temperature perturbatively with either the time-independent degenerate perturbation theory [52] or the Matsubara imaginary time formalism [53,54]. However, it is unclear whether results obtained through the Matsubara formalism hold at very low temperatures. The time-independent perturbation method does not suffer from such limitation, which is why we focus on this method in the main text, with further details given in Appendix B 1. The derivation of the correlation function using the Matsubara formalism can be found in Appendix B 2. When Eqs. (39) and (40) hold, the single-junction correlation function reads

$$G_\alpha(t) = \frac{\lambda_\alpha^2}{2}e^{-iE_{\rm C\alpha}t} + O\big(\lambda_\alpha^3, e^{-\beta E_{\rm C\alpha}}\big). \tag{41}$$

Note that Eq. (41) is dramatically different from Eq. (32) as the characteristic oscillation frequency in Eq. (41) is $E_{C\alpha}$ instead of $\sqrt{E_{J\alpha}E_{C\alpha}}$. This substantial difference is due the fact that they are valid in two opposite regimes. The first frequency represents the energy necessary to add a charge on a capacitor, while the second one defines the plasma (resonance) frequency due to sound modes in the JJA.

1. Derivation of the single-junction correlation function through time-independent perturbation method

We now derive the correlation function in the limit of large charging energy for a single Josephson junction so we can drop the subscript α. The corresponding Hamiltonian is $H = H_C + \lambda H_J$, where $\lambda = E_J/E_C \ll 1$ and

$$H_C = E_C N^2, \tag{42}$$

$$H_J = -E_C \cos\varphi. \tag{43}$$

We consider time-independent perturbation theory treating the Josephson Hamiltonian as a perturbation. In this framework, we compute the average values in the correlation function explicitly using the eigenenergies and eigenstates obtained from our perturbative calculation.

As pointed out earlier, the Hamiltonian H is invariant under charge conjugation, $\mathscr{C}H\mathscr{C} = H$, which yields $[H, \mathscr{C}] = 0$. As such, H and $\mathscr{C}$ share a common eigenbasis. Since $\mathscr{C}^2 = 1$, the eigenvalues of $\mathscr{C}$ are ± 1, which means that the corresponding eigenstates are either symmetric or antisymmetric under charge conjugation. We consequently denote by $|\psi_{n,\pm}\rangle$ the common eigenstates of H and $\mathscr{C}$ such that

$$H\,|\psi_{n,\pm}\rangle = E_{n,\pm}\,|\psi_{n,\pm}\rangle\,, \tag{44}$$

$$\mathscr{C}\,|\psi_{n,\pm}\rangle = \pm\,|\psi_{n,\pm}\rangle\,, \tag{45}$$

where the index n is a positive integer that labels the energy levels of the charging Hamiltonian H_C. Working in this basis, the single-junction correlation function $G(t) = \langle N(t)N(0)\rangle$ is expressed as

$$G(t) = \frac{1}{Z}\sum_{m,n,\pm} |\langle\psi_{m,\pm}|N|\psi_{n,\mp}\rangle|^2 e^{-\beta E_{m,\pm}} e^{i(E_{m,\pm}-E_{n,\mp})t}, \tag{46}$$

with the partition function

$$Z = \sum_{n,\pm} e^{-\beta E_{n,\pm}}. \tag{47}$$

One should note that, since the number operator N is odd under charge conjugation, it only couples states of different charge parities. This is why we only have to consider scalar products of the type $\langle\psi_{m,\pm}|N|\psi_{n,\mp}\rangle$ in Eq. (46).

Let us now compute the eigenstates $|\psi_{n,\pm}\rangle$ and eigenenergies $E_{n,\pm}$ to lowest orders in λ using time-independent perturbation theory [52]. The starting point is to write $E_{n,\pm}$ and $|\psi_{n,\pm}\rangle$ as power series in λ,

$$E_{n,\pm} = \sum_{q=0}^{\infty} \lambda^q E^{(q)}_{n,\pm}, \tag{48}$$

$$|\psi_{n,\pm}\rangle = \sum_{q=0}^{\infty} \lambda^q \left|\psi^{(q)}_{n,\pm}\right\rangle. \tag{49}$$

Equating the two sides of Eq. (44) to all orders in λ then yields

$$H_C\left|\psi^{(q)}_{n,\pm}\right\rangle + H_J\left|\psi^{(q-1)}_{n,\pm}\right\rangle = \sum_{p=0}^{q} E^{(p)}_{n,\pm}\left|\psi^{(q-p)}_{n,\pm}\right\rangle. \tag{50}$$

To the zeroth order in λ, we simply obtain

$$H_C\left|\psi^{(0)}_{n,\pm}\right\rangle = E^{(0)}_{n,\pm}\left|\psi^{(0)}_{n,\pm}\right\rangle. \tag{51}$$

This means that $E^{(0)}_{n,\pm}$ is an eigenenergy of H_C, with $|\psi^{(0)}_{n,\pm}\rangle$ being the corresponding eigenstate. While we can readily identify $E^{(0)}_{n,\pm}$ with the charging energy, $E^{(0)}_{n,\pm} = n^2 E_C$, the state $|\psi^{(0)}_{n,\pm}\rangle$ remains undetermined at this stage. This is because all the energy levels of the charging Hamiltonian except the ground state are twofold degenerate, and Eq. (51) then only tells us that $|\psi^{(0)}_{n,\pm}\rangle$ belongs to the subspace generated by the charge states $|n\rangle$ and $|-n\rangle$. However, since each state $|\psi_{n,\pm}\rangle$ has a definite charge parity—we recall that it is an eigenstate of both H and $\mathscr{C}$—, all the corrections $|\psi^{(q)}_{n,\pm}\rangle$ must have the same property. This includes the zeroth order eigenstates which must also satisfy $\mathscr{C}\,|\psi^{(0)}_{n,\pm}\rangle = \pm\,|\psi^{(0)}_{n,\pm}\rangle$. For all $n > 0$, we then find the appropriate choice for these states to be

$$\left|\psi^{(0)}_{n,\pm}\right\rangle = |\chi_{n,\pm}\rangle \equiv \frac{1}{\sqrt{2}}(|n\rangle \pm |-n\rangle), \tag{52}$$

where $\mathscr{C}\,|\chi_{n,\pm}\rangle = \pm\,|\chi_{n,\pm}\rangle$. Hence, each twofold degenerate charge energy level can be further subdivided into two eigenstates of different charge parities; we expect the degeneracy of these states to be lifted by the Josephson Hamiltonian. Finally, one should note that the relevant zeroth order eigenstate for $n = 0$ is simply $|\psi^{(0)}_0\rangle = |0\rangle$, which indicates that the ground state $|\psi_0\rangle$ is even under charge conjugation.

Using Eq. (50) with $q = 1$, we find the corrections to the energy to first order in λ,

$$E^{(1)}_{n,\pm} = \left\langle\psi^{(0)}_{n,\pm}\middle|H_J\middle|\psi^{(0)}_{n,\pm}\right\rangle. \tag{53}$$

The Josephson potential only couples neighboring charge states as, for any charge states $|m\rangle$ and $|n\rangle$, we have

$$\langle m|H_J|n\rangle = -\frac{E_C}{2}(\delta_{m,n+1} + \delta_{m,n-1}). \tag{54}$$

Thus, the perturbation does not yield any correction to the energies to first order in λ, $E^{(1)}_{n,\pm} = 0$.

The first-order eigenstates are given by

$$\left|\psi^{(1)}_{n,\pm}\right\rangle = -\sum_{m\neq n} \frac{\left\langle\psi^{(0)}_{m,\pm}\middle|H_J\middle|\psi^{(0)}_{n,\pm}\right\rangle}{(m^2-n^2)E_C}\left|\psi^{(0)}_{m,\pm}\right\rangle. \tag{55}$$

Note that here the norm and phase of $|\psi_{n,\pm}\rangle$ have been chosen such that $\langle\psi_{n,\pm}|\psi_{n,\pm}\rangle = 1$ and $\langle\psi^{(0)}_{n,\pm}|\psi_{n,\pm}\rangle$ be real. To first order in λ, this imposes $\langle\psi^{(0)}_{n,\pm}|\psi^{(1)}_{n,\pm}\rangle = 0$. In what follows, the cases for $n = 0$ or $n = 1$ must be treated separately since they involve the ground state which is clearly distinct from the excited states as regards the structure of their leading-order terms. Namely, we have $|\psi^{(0)}_0\rangle = |0\rangle$ while, for $n > 0$, $|\psi^{(0)}_{n,\pm}\rangle = |\chi_{n,\pm}\rangle$. For $n = 0$, we obtain

$$|\psi_0\rangle = |0\rangle + \frac{\lambda}{\sqrt{2}}\,|\chi_{1,+}\rangle + O(\lambda^2). \tag{56}$$

For $n = 1$, we find

$$|\psi_{1,+}\rangle = |\chi_{1,+}\rangle + \frac{\lambda}{6}|\chi_{2,+}\rangle + \frac{\lambda}{\sqrt{2}}|0\rangle + O(\lambda^2), \quad (57)$$

$$|\psi_{1,-}\rangle = |\chi_{1,-}\rangle + \frac{\lambda}{6}|\chi_{2,-}\rangle + O(\lambda^2). \quad (58)$$

Finally, for $n > 1$, we have

$$|\psi_{n,\pm}\rangle = |\chi_{n,\pm}\rangle + \frac{\lambda}{4n+2}|\chi_{n+1,\pm}\rangle - \frac{\lambda}{4n-2}|\chi_{n-1,\pm}\rangle + O(\lambda^2). \quad (59)$$

We now consider the second-order corrections to the energy. According to Eq. (50) with $q = 2$, we have

$$E^{(2)}_{n,\pm} = -\sum_{m\neq n} \frac{\left|\langle\psi^{(0)}_{m,\pm}|H_J|\psi^{(0)}_{n,\pm}\rangle\right|^2}{(m^2-n^2)E_C}. \quad (60)$$

For $n = 0$, this yields

$$E_0 = -\frac{\lambda^2 E_C}{2} + O(\lambda^3). \quad (61)$$

For $n = 1$, we obtain

$$E_{1,+} = E_C\left(1 + \frac{5\lambda^2}{12}\right) + O(\lambda^3), \quad (62)$$

$$E_{1,-} = E_C\left(1 - \frac{\lambda^2}{12}\right) + O(\lambda^3). \quad (63)$$

The Josephson Hamiltonian thus lifts the degeneracy of the first excited eigenstates to second order in λ. Conversely, higher-energy excited states remain degenerate to this point as, for $n > 1$, we find

$$E_{n,\pm} = E_C\left(n^2 + \frac{\lambda^2}{2(4n^2-1)}\right) + O(\lambda^3). \quad (64)$$

We can now use the result obtained with the perturbation method to compute the single-junction correlation function in Eq. (46). However, the eigenenergies only appear in oscillating exponentials multiplied by the time t or in the Boltzmann factors multiplied the inverse temperature β in Eq. (46). This must be accounted for in subsequent calculations as one has to ensure that energy corrections to high orders in λ can still be neglected. This is clearly the case if we restrict ourselves to short times, $t \ll 1/(\lambda^2 E_C)$. This limitation to short times does not constitute a hindrance to our analysis. Indeed, we are interested here in situations where the correlation function for the whole chain rapidly decays so that the Born–Markov approximations hold. The crucial point of our calculation is to ensure that this fast decay does happen, and we do not need to resolve the dynamics of correlations for longer times. Therefore, we will only consider the short-time regime $t \ll 1/(\lambda^2 E_C)$ hereafter. Overall, our approach provides a satisfactory description of correlations in a single junction, so long as $\omega_B^{-1} \ll 1/(\lambda^2 E_C)$, where ω_B^{-1} is the correlation time for the whole chain. We typically estimate $\omega_B \sim \delta E_C$, where δE_C is the width of the charging energy distribution across the chain, as shown in Eq. (74) later. This results in the constraint $E_J \ll \sqrt{E_C \delta E_C}$ in Eq. (39). A more accurate estimate of ω_B for a specific example will be derived in Eq. (99) later.

As regards the Boltzmann factors, we will actually consider two opposite regimes of temperature in what follows. First, we analyze the regime of high temperatures, $\beta^{-1} \gg \lambda^2 E_C$. This is in the same spirit as the limitation to short times discussed above. In this regime, terms to high orders in λ can be neglected in the Boltzmann factors so our perturbative results can be used. Then, in a second time, we tackle the low-temperature regime. In this case, we cannot estimate the Boltzmann factors with accuracy through a series in powers of λ. However, if the temperature is low enough, then we can only keep the contribution of the ground state to the correlation function. This is because the Boltzmann factors corresponding to excited states, $e^{-\beta E_{n,\pm}}$ with $n > 0$, are negligible with respect to $e^{-\beta E_0}$, which is typically the case when $\beta^{-1} \ll E_C$. Then, the Boltzmann factors $e^{-\beta E_0}$ in the numerator and the denominator cancel each other so it is not necessary to have the full expansion for the energy E_0.

Let us first analyze the regime of high temperatures where $\beta^{-1} \gg \lambda^2 E_C$. For simplicity, we only keep terms to leading order in λ, $E_{n,\pm} = n^2 E_C + O(\lambda^2)$ and $\langle\psi_{m,\pm}|N|\psi_{n,\mp}\rangle = m\delta_{mn} + O(\lambda)$ (recall that N only couples states of different charge parities). In this context, we find that the single-junction correlation reduces to that of a free rotor,

$$G(t) \approx \frac{2\sum_{n=1}^{\infty} n^2 e^{-n^2\beta E_C}}{1 + 2\sum_{n=1}^{\infty} e^{-n^2\beta E_C}}, \quad (65)$$

where we recall that the short-time limit, $t \ll 1/(\lambda^2 E_C)$, is considered here. The factors of 2 above illustrate that excited states of different parities contribute equally to the correlation function.

We now turn to the opposite low-temperature regime where $\beta^{-1} \ll E_C$. In this case, we only keep the terms in Eq. (46) whose Boltzmann factor is associated to the ground state. The correlation function then reads

$$G(t) \approx \sum_{n=1}^{\infty} |\langle\psi_0|N|\psi_{n,-}\rangle|^2 e^{-i(E_{n,-}-E_0)t}. \quad (66)$$

Again, N only couples states of different charge parities and $|\psi_0\rangle$ is even under charge conjugation, which is why the sum above only features the odd eigenstates $|\psi_{n,-}\rangle$. Moreover, since $N|0\rangle = 0$, we deduce that the term of zeroth order in λ vanishes here. To leading-order in λ, only $|\psi_{1,-}\rangle$ contributes to the sum, so that we find, for $t \ll 1/(\lambda^2 E_C)$,

$$G(t) \approx \frac{\lambda^2}{2} e^{-iE_C t}. \quad (67)$$

We observe two clearly different dynamics for correlations in Eqs. (65) and (67). In the high temperature regime, we find that the correlation function is constant. This rules out the possibility for the whole chain's correlation function to decay fast and forbids Markovianity. Crucially, in the case of free rotors ($\lambda = 0$), the dynamics of the correlation function is always given by this constant term so the Born–Markov approximation never applies. On the contrary, Eq. (67) features an exponential oscillating in time. We will show later that this time dependence can give rise to a rapidly decaying correlation function for the whole chain to leading order provided that the charging energy distribution along the chain is appropriately chosen. This underlines the primary importance

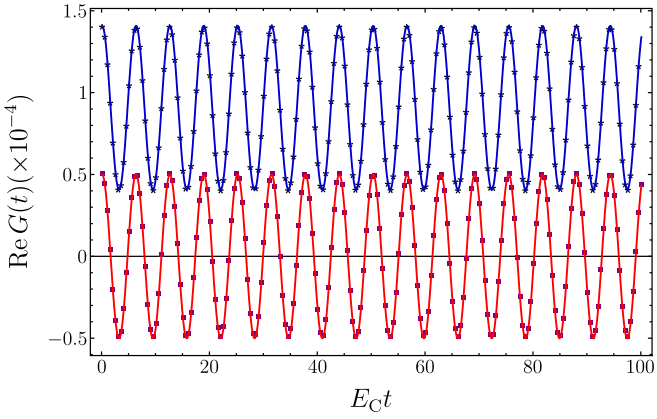

FIG. 2. Check of $G(t)$ against numerical calculation. The value of the Josephson energy is $E_J = 0.01E_C$. The red solid and blue dotted lines are analytical calculations of the real parts of $G(t)$ at temperatures $\beta^{-1} \ll E_C/\ln(E_C/E_J) = 0.2E_C$ and $\beta^{-1} = 0.1E_C$, respectively, which are plotted according to Eq. (68). The purple squares and black stars are the corresponding numerical calculations of the real parts of $G(t)$ for these two temperatures. We clearly see that the perturbative results from Eq. (68) are in excellent agreement with the numerical results for $t \ll 1/(\lambda^2 E_C) = 10^4/E_C$. Furthermore, the constant offset in $G(t)$, i.e., the second term in the right-hand side of Eq. (68), which becomes nonnegligible at temperature $\beta^{-1} \sim E_C/\ln(E_C/E_J)$, is also confirmed by the numerical calculations.

of the Josephson potential as it introduces an overlap between the ground state $|\psi_0\rangle$ and the even charge eigenstate $|\chi_{1,+}\rangle$ as shown in Eq. (66). This overlap gives rise to the oscillating behavior of the correlation function, which is the leading-order behavior in the low-temperature regime. In summary, we observe that the Josephson junction chain can behave as a Markovian bath at low temperature while this is no longer the case for higher temperatures. Here, Markovianity breaks down as temperature increases contrary to what is usually witnessed in the usual harmonic bath, where the short correlation time at high temperature guarantees Markovianity, as one can see from Eq. (34).

In the low-temperature regime, only the ground state's contribution to correlations have been taken into account when moving from Eq. (46) to Eq. (66). When temperature is increased, contributions from excited states must also be taken into consideration. In doing so, the transition in the dynamics of correlation from oscillatory to constant can be analyzed more thoroughly. For example, when $e^{-\beta E_C} \sim \lambda^2$, that is $\beta^{-1} \sim E_C/(-\ln\lambda)$, it is necessary to include the contribution from the first excited states into the calculation. We then obtain

$$G(t) \approx \frac{\lambda^2}{2} e^{-iE_C t} + 2e^{-\beta E_C}. \tag{68}$$

This expression provides a satisfactory description of single-junction correlation function for short times, $t \ll 1/(\lambda^2 E_C)$, and moderately low temperatures, $\lambda^3 E_C \ll \beta^{-1} \ll E_C$. This justifies a posteriori the form of Eq. (40) refining the regime of validity of Eq. (67). Figure 2 shows that Eq. (68) can characterize the dynamics for $t \ll 1/(\lambda^2 E_C)$ with excellent precision and the constant offset corresponding to the second term in the right-hand side of Eq. (68) is confirmed by the numerics. The simulation is performed by numerically calculating $\langle N(t)N(0)\rangle$ taking into account the first 41 charge eigenbasis states, namely, the states $|n\rangle$ for $n = -20, \ldots, 20$.

More details about the perturbative calculation of the single-junction correlation function are given in Appendix B 1.

2. *JJA correlation function in the continuum limit*

When temperature is further lowered such at Eq. (40) is satisfied, the subleading order is much smaller than the leading order in Eq. (68). Therefore, it reduces to Eq. (41). In this regime, the Josephson bath correlation function obtained from Eq. (41) is

$$\Gamma(t) = \sum_\alpha \frac{g_\alpha^2 E_{J\alpha}^2}{2E_{C\alpha}^2} e^{-iE_{C\alpha}t} = \frac{1}{2}\left(\frac{\varepsilon_I}{e}\right)^2 \sum_\alpha E_{J\alpha}^2 e^{-iE_{C\alpha}t}, \tag{69}$$

where we have used the explicit Eq. (18) for g_α in the last equality. In the continuum limit, this becomes

$$\Gamma(t) = \frac{1}{2}\left(\frac{\varepsilon_I}{e}\right)^2 \int dx \nu(x)[E_J(x)]^2 e^{-iE_C(x)t}. \tag{70}$$

We emphasize that x and $\nu(x)$ in Eq. (70) have their own meaning depending on the specific context of how the JJA bath is built. We will come back their exact meaning when we discuss specific examples in Sec. VI. Here, one can simply view x as the index for the modes of the JJA and $\nu(x)$ is the degeneracy of the mode of $E_C(x)$. Furthermore, we note that Eq. (70) is valid if the continuous versions of Eqs. (39) and (40) hold. Namely, for all x, we must have

$$E_J(x) \ll E_C(x),\ \sqrt{E_C(x)\delta E_C}, \tag{71}$$

$$\beta^{-1} \ll \Delta_* \equiv \min_x \Delta(x), \tag{72}$$

where δE_C is the width of the distribution of the charging energy across the chain and

$$\Delta(x) \equiv E_C(x)/[-\ln\lambda(x)]. \tag{73}$$

We deem the junction at position x to be in *the zero-temperature limit* if $\beta^{-1} \ll \Delta(x)$. Then, the whole chain is in the zero-temperature limit if all junctions are, that is if Eq. (72) is satisfied.

We change variables in Eq. (70) to obtain

$$\Gamma(t) = \left(\frac{\varepsilon_I}{2e}\right)^2 \int_0^\infty dE_C J(E_C) e^{-iE_C t}, \tag{74}$$

where

$$J(E_C) \equiv 2\sum_k \nu_k(E_C)\left[E_J^{(k)}(E_C)\right]^2 \left|\frac{dx_k}{dE_C}(E_C)\right|. \tag{75}$$

Here k labels the intervals I_k on which $E_C(x)$ is monotonic so that the inverse function $x_k(E_C)$ is properly defined, and

$$\nu_k(E_C) \equiv \nu(x_k(E_C)), \tag{76}$$

$$E_J^{(k)}(E_C) \equiv E_J(x_k(E_C)). \tag{77}$$

Comparing to Eq. (34), we notice that $J(E_C)$ plays a similar role to that of the spectral density in the harmonic regime,

accounting for the decay of the correlation function. Roughly speaking, $\Gamma(t)$ will decay on a timescale of the order of the width of $J(E_C)$ since $\Gamma(t)$ is the "half Fourier transform" of $J(E_C)$ as seen in Eq. (74). Then, if we denote by δE_C the width of $J(E_C)$, the characteristic decay time of $\Gamma(t)$ will approximately be $1/\delta E_C$.

IV. TEMPERATURE-DRIVEN TRANSITION TO NON-MARKOVIANITY

When temperature is much smaller than the charging energy but violates Eq. (40), the single-junction correlation function is given by Eq. (68) rather than Eq. (67). This is because the next-to-leading order term $e^{-\beta E_C}$ becomes comparable to the leading-order term. In the continuum limit, this term contributes to a constant offset to the correlation function when the bath temperature reaches the point $\beta^{-1} \sim \Delta_*$, but $\beta^{-1} \ll \min_x E_C(x)$. Thus, the Josephson bath correlation function no longer decays in this regime, meaning that the dynamics of the system becomes non-Markovian. The presence of this constant offset can be intuitively understood considering that in the regime we analyze, charge fluctuations in the Josephson chain are long-lived due to the small value of the Josephson energy (the commutator of the charge operator N_α with the chain Hamiltonian is very small). When the constant offset is nonnegligible, one can expect that correlations between the state of the system and the bath built up by the interaction never completely decay, which invalidates the GKSL treatment. To understand when this happens, we use Eqs. (18) and (28), to calculate the constant offset,

$$\Gamma_0 = 2\left(\frac{\varepsilon_I}{e}\right)^2 \int dx\, \nu(x) E_C^2(x) e^{-\beta E_C(x)}. \tag{78}$$

However, the magnitude of the constant offset will depend on the spatial variation of $\Delta(x)$: We denote the place where $\Delta(x)$ reaches its minimum Δ_* as x_*. When the temperature of the chain β^{-1} becomes comparable to Δ_*, obviously the offset will contribute to the single-junction correlation function for junctions near $x = x_*$. If the spatial variation of the $\Delta(x)$ is small, i.e., $\max_x |\Delta(x) - \Delta_*|$ is not too much larger than Δ_*, then the offset will contribute to a significant portion of the single-junction correlation functions across the chain, not just for junctions near $x = x_*$ so that the overall bath correlation functions is significantly shifted.

However, if the spatial variation of $\Delta(x)$ is relatively large, then it may happen that only a small portion of the chain near $x = x_*$ surpasses the zero-temperature limit when β^{-1} becomes comparable to Δ_*. When this is the case, the offset of the bath correlation function may be small compared to the magnitude of the one in the zero-temperature limit, or even negligible.

We will discuss this phenomenon again for a concrete example with effective Lorentz spectral density in Sec. VI A.

V. THE GKSL MASTER EQUATION AND BATH DUALITY

A. The decay rate and Lamb shift

We now discuss the dynamics of the LC oscillator that is weakly and capacitively coupled to the Josephson bath, shown in the dotted box in Fig. 1(a). When the correlation function $\Gamma(t)$ decays fast, the system dynamics may be described by a GKSL master equation. Combined with the results of previous section, it requires δE_C be large enough, which can come from reservoir engineering or disorder of the charging energy (see Sec. VI). When this is the case, we can perform the Born–Markov approximation and the secular approximation [3,4], to find the following (interaction picture) Markovian master equation for the LC oscillator shown in the dotted box in Fig. 1(a):

$$\frac{d\rho_S}{dt} = -i[H_{LS}, \rho_S(t)] + \kappa(\omega_0)\mathcal{D}[b]\rho_S(t). \tag{79}$$

Here ω_0 is defined in Eq. (21), $H_{LS} = \delta_{LS}(\omega_0) b^\dagger b$ is the Lamb shift Hamiltonian that accounts for the renormalization of the LC oscillator's energy levels due to the coupling to the JJA bath, while the dissipator $\mathcal{D}[b]\rho_S(t) \equiv b^\dagger \rho_S(t) b - \{\rho_S(t), b^\dagger b/2\}$ describes the equilibration of the oscillator with the bath through the emission of photons at frequency ω_0. The Lamb shift $\delta_{LS}(\omega_0)$ and the emission rate $\kappa(\omega_0)$ are both deduced from the Fourier transformed correlation function $\Gamma(\omega_0)$,

$$\delta_{LS}(\omega_0) = -\frac{C\omega_0}{2}\mathrm{Im}[\Gamma(\omega_0) + \Gamma(-\omega_0)], \tag{80}$$

$$\kappa(\omega_0) = C\omega_0 \mathrm{Re}\Gamma(\omega_0), \tag{81}$$

$$\Gamma(\omega_0) = \int_0^\infty dt \Gamma(t) e^{i\omega_0 t}. \tag{82}$$

A brief derivation of the GKSL master equation is presented in Appendix A. Let us now calculate the Lamb shift and decay rate stemming from the JJA bath correlation function given in Eq. (74). The half Fourier transform yields

$$\Gamma(\omega) = \left(\frac{\varepsilon_I}{2e}\right)^2 \left[\pi J(\omega)\Theta(\omega) - i\mathcal{P}\int_0^\infty dE_C \frac{J(E_C)}{E_C - \omega}\right], \tag{83}$$

where $\Theta(\omega)$ is the Heaviside function and $\mathcal{P}$ denotes the Cauchy principal value. We then straightforwardly obtain the Lamb shift,

$$\delta_{LS}(\omega_0) = \frac{\omega_0 \varepsilon_I^2}{16 E_Q}\mathcal{P}\int_0^\infty dE_C J(E_C)\left(\frac{1}{E_C - \omega_0} + \frac{1}{E_C + \omega_0}\right), \tag{84}$$

where we have introduced $E_Q = e^2/(2C)$, the renormalized charging energy of the LC oscillator. Finally, the decay rate reads

$$\kappa(\omega_0) = \frac{\pi \varepsilon_I^2 \omega_0 J(\omega_0)}{8 E_Q}, \tag{85}$$

which is the rate of emission of a photon at frequency ω_0 by the LC oscillator. The rate for the opposite process, where the oscillator is excited by the absorption of a photon vanishes here. This indicates that the JJA bath is effectively at zero temperature: The oscillator cannot absorb any photon if the bath emits none.

B. Bath duality

From Eqs. (38) and (74), it is clear that the zero-temperature correlation function of the JJA bath takes similar forms whether E_J or E_C defines the largest energy scale in the problem, leading to similar effects on the system's dynamics.

TABLE I. Parameter correspondence between the large E_C regime and large E_J regime at the zero temperature limit, where the leading order correlation function of JJA bath produces the same coarse-grained dynamics for the primary LC oscillator. The parameters in the large E_J regime come with tildes to distinguish those in the large E_C regime. The basic variable on the left column is E_C while the one on the right column is $\tilde{\omega}$.

Large E_C limit $E_J(x) \ll E_C(x)$	Large E_J limit $\tilde{E}_C(x) \ll \tilde{E}_J(x)$
Zero-temperature limit $\beta^{-1} \ll \Delta_*$	Zero-temperature limit $\tilde{\beta}^{-1} \ll \min_x \tilde{\omega}(x)$
$x_k \in I_k$	$x_k \in I_k$
$E_C(x_k)$	$\tilde{\omega}(x_k) \equiv \sqrt{2\tilde{E}_C(x_k)\tilde{E}_J(x_k)}$
$\nu_k(E_C)$	$\tilde{\nu}_k(\tilde{\omega})$
$2\left[E_J^{(k)}(E_C)\right]^2/E_C$	$\tilde{E}_C^{(k)}(\tilde{\omega})$

The only difference between the two regimes is then how the spectral density, and therefore the damping rate and Lamb shift, are related to the microscopic parameters of the JJA.

We found that the spectral densities in the two regimes can be mapped onto each other, e.g., through the parameter correspondence list in Table I. The existence of such mapping implies that there exist two sets of parameters, $(E_J(x), E_C(x))$ in the large E_C regime and $(\tilde{E}_J(x), \tilde{E}_C(x))$ in the large E_J regime, linked by the relation in Table I, which lead to the same coarse-grained dynamics for any small system coupled to the JJA, i.e., the same form of GKSL master equation and the same value of the coefficients. We dub the mapping the between the two regimes as *bath duality*.

Let us now illustrate how the bath duality is actually performed. The parameters in the large E_J regime come with tildes to distinguish them from those in the large E_C regime. Moreover, the parameter $E_C(x_k)$ in the left column plays the same role as the frequency $\tilde{\omega}_k$ in the right column.

To obtain the same dynamics, one can ensure that the value of $E_C(x_k)$ (second row of the table) is the same as that of $\tilde{\omega}(x_k)$, that the function $\nu_k(E_C) = \nu(x_k(E_C))$ (third row) takes the same values as $\tilde{\nu}_k(\tilde{\omega}) = \tilde{\nu}(x_k(\tilde{\omega}))$, and finally that $2\{E_J^{(k)}(E_C)\}^2/E_C = 2\{E_J(x_k(E_C))\}^2/x_k(E_C)$ (last row of the table) equals $\tilde{E}_C^{(k)}(\tilde{\omega}) = \tilde{E}_C(x_k(\omega))$.

From this correspondence rules, we find

$$\tilde{E}_C(x_k) = \frac{2E_J^2(x_k)}{E_C(x_k)}, \tag{86}$$

and

$$\tilde{E}_J(x_k) = \frac{\tilde{\omega}^2(x_k)}{2\tilde{E}_C(x_k)} = \frac{\tilde{\omega}^3(x_k)}{4E_J^2(x_k)} = \frac{E_C^3(x_k)}{4E_J^2(x_k)}, \tag{87}$$

using the identification of $\tilde{\omega}(x_k)$ with $E_C(x_k)$. This leads to the relation

$$\tilde{E}_C(x_k)/\tilde{E}_J(x_k) \sim [E_J(x_k)/E_C(x_k)]^4 \ll 1, \tag{88}$$

which shows the mapping indeed connects the large E_C regime to the large E_J regime. Furthermore, one can also check that the mapping preserves the zero-temperature limit

$$\tilde{\beta} \ll \tilde{\omega}(x_k), \quad \forall x_k \in I_k, \tag{89}$$

as along as the temperature for the large E_J regime is taken as

$$\tilde{\beta}^{-1} \lesssim \ln\left[E_C(x)/E_J(x)\right]_{\min}\beta^{-1}. \tag{90}$$

An example of how this mapping can be implemented will be discussed in next section.

VI. EXAMPLES

In this section, we will give two concrete examples illustrating how the result in Sec. V can be applied. Practically, we know [55]

$$E_{C\alpha} = \frac{2e^2 w_\alpha}{\epsilon_r A_\alpha}, \tag{91}$$

$$E_{J\alpha} = \frac{F_J A_\alpha}{\zeta \sinh(w_\alpha/\zeta)}, \tag{92}$$

where w_α and ϵ_r are the thickness and dielectric constant of the oxidation material, A_α is the area of the junctions, F_J is a constant that depends on the density of the cooper pairs on the islands which has the dimension of a force, and ζ is a constant that depends on the tunneling barrier that has the dimension of a length. Below, we will consider variations of the oxidation material thickness and of the junction area across the chain, all other parameters being kept fixed.

In the first example, the junction density and the junction area distribution are properly engineered such that the effective spectral density is Lorentzian, a case frequently studied in the field of open quantum systems. In the second example, we discuss a common case in condensed matter physics where the JJA presents disorder in the values of the charging and Josephson energies caused by the Gaussian disorder of the width of the oxidation material. It should be noted that in the first example the spatial dependences of the charging and Josephson energies on the junction position are known, while in the second example these energies at each junction are random and correlated through the width of the oxidation material.

A. Engineering the areas of the junctions

$$E_C(x) = \left(1 + \frac{ax^2}{2L^2}\right)E_{C0}, \tag{93}$$

where $a > 0$ is dimensionless quantity characterizing the variation of the charging energy across the chain, $x \in [-L, L]$. According to Eqs. (91) and (92), the distribution of E_J across the chain is

$$E_J(x) = E_{J0}\left(1 + \frac{ax^2}{2L^2}\right)^{-1}, \tag{94}$$

where

$$E_{J0} = \frac{2e^2 F_J w}{\epsilon_r \zeta E_{C0} \sinh(w/\zeta)}. \tag{95}$$

To satisfy the large E_C condition in Eq. (71), we require $E_{C0} \gg E_{J0}$. The junctions are assumed to be distributed

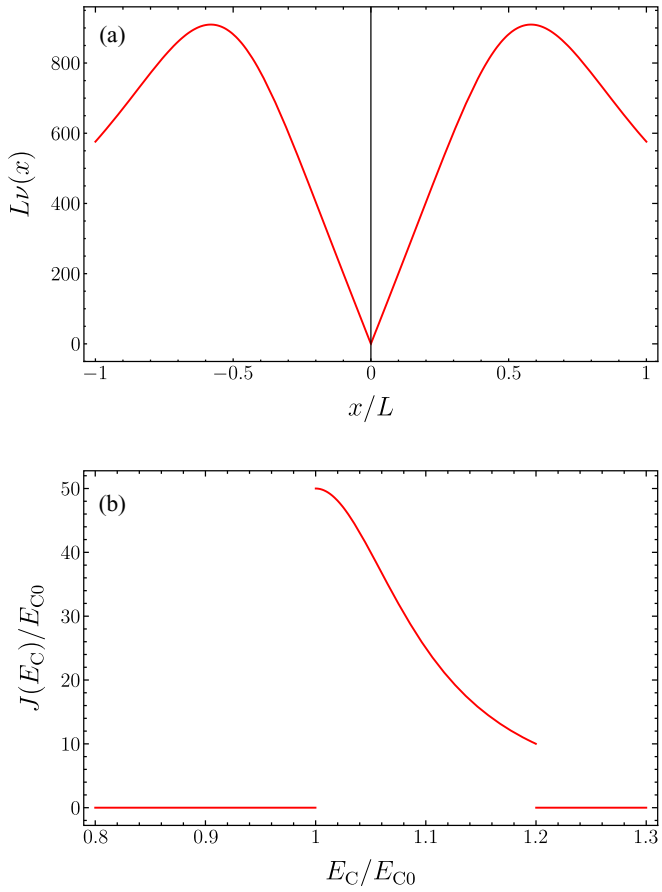

FIG. 3. (a) The junction density given by Eq. (96), (b) the spectral density given by Eq. (97), which is nonvanishing only in the range of characteristic frequencies of the Josephson bath, i.e., $[E_{C0},\ (1+a/2)E_{C0}\ ]$. Value of parameters: $\mathcal{A}=500$, $\sigma=0.25$, $a=0.4$, $E_{J0}=0.05E_{C0}$. The total number of the junction is the JJA is roughly $N_J=\int_{-L}^{L}\mathrm{d}x\,\nu(x)\approx 1277$.

according to the junction density

$$\nu(x)=\frac{\mathcal{A}L^2|x|}{x^4+4\sigma^2L^4}\left(1+\frac{ax^2}{2L^2}\right)^2, \tag{96}$$

where the dimensionless quantities $\mathcal{A}$ and σ, respectively, characterize the amplitude and variation of the junction density across the chain. The junction density $\nu(x)$ accounts for the weights of a junction with parameter $E_C(x)$ and $E_J(x)$, similarly to the concept of density of states accounting for the degeneracy of energy levels. The shape of $\nu(x)$ is shown in Fig. 3(a). Then, according to Eq. (75),

$$J(E_C)=\frac{a\mathcal{A}E_{C0}E_{J0}^2}{(E_C-E_{C0})^2+(a\sigma E_{C0})^2}, \tag{97}$$

when $E_{C0}\leqslant E_C\leqslant(1+a/2)E_{C0}$, and $J(E_C)=0$ otherwise. The plot of $J(E_C)$ is shown in Fig. 3(b).

To justify the Born–Markov and secular approximations, the following conditions must be satisfied:

$$\kappa(\omega_0)\ll\omega_B,\omega_0, \tag{98}$$

where ω_B^{-1} is the timescale, on which the JJA bath correlation function $\Gamma(t)$ decays.

Now we derive an *empirical* rule for the above example, under which Eq. (98) can be satisfied. Similar rules can be analogously derived for other distributions of the junction density and parameters. According to Eq. (74), one can roughly regard $\Gamma(t)$ as the Fourier transform of $J(E_C)$, although, strictly speaking, it is "the half Fourier transform" $J(E_C)$. Therefore, the decay rate of $\Gamma(t)$ should be the width of $J(E_C)$, i.e.,

$$\omega_B\sim\delta E_C\equiv aE_{C0}\min\left\{\sigma,\frac{1}{2}\right\}. \tag{99}$$

According to Eqs. (85) and (97), the maximum decay rate is obtained for $\omega_0=E_{C0}\sqrt{1+(a\sigma)^2}$, with $\kappa_{\max}=\zeta_M E_{C0}(1+\sqrt{1+(a\sigma)^2})/2$, where

$$\zeta_M\equiv\frac{\pi\mathcal{A}\varepsilon_I^2E_{J0}^2}{8a\sigma^2E_{C0}E_Q} \tag{100}$$

characterizes the Markovianity of the chain. The maximum ratio between $\kappa(\omega_0)$ and ω_0 occurs when $\omega_0=E_{C0}$, where $[\kappa(\omega_0)/\omega_0]_{\max}=\zeta_M$. Therefore, Eq. (98) can be satisfied if

$$\frac{\zeta_M[1+\sqrt{1+(a\sigma)^2}]}{a\sigma}\ll 1,\ 2\sigma, \tag{101}$$

$$\zeta_M\ll 1. \tag{102}$$

It turns out that Eqs. (101) and (102) are satisfied when ζ_M is small enough. In such a case, the JJA behaves as a Markovian bath. In Fig. 4, one can see that for the given parameters for the JJA and the LC oscillator, Eqs. (101) and (102) are satisfied so that the validity of the GKSL master equation is justified. From Figs. 4(a) and 4(b), we observe that the Josephson bath correlation time ω_B^{-1} is roughly about $10/\delta E_C$ and $\kappa/\omega_B\sim 10^{-4}$–$10^{-3}$. Thus, within the GKSL weak-coupling approach, the coupling that the circuit QED setup here has achieved is already much larger compared to the atomic case where [3,4] $\kappa/\omega_B\sim 10^{-7}$–$10^{-6}$.

Note that the Markovian property of the Josephson bath, where the correlation function decays faster than the LC oscillator, as shown in Fig. 4(a), only holds in the zero-temperature limit given by Eq. (72). As we have discussed in Sec. IV, when the temperature of the chain is comparable to Δ_* defined in Eq. (72), non-Markovian dynamics may occur due to the significant constant offset in the Josephson bath correlation function. For the charging energy distribution in Eq. (93), Δ_* is $E_{C0}/\ln(E_{C0}/E_{J0})$, which is reached at the origin. The magnitude of the offset depends on the spatial variation of $\Delta(x)$ defined in Eq. (73): The flatter the spatial distribution, the larger the offset. The correlation function for cases with small and large spatial variation of $\Delta(x)$ are given in Figs. 5 and 6, respectively. One can easily find that for $\beta^{-1}=0.33\Delta_*$ and $\beta^{-1}=0.42\Delta_*$, the portion in the JJA near the origin in Fig. 5(b) that surpasses the zero-temperature limit is larger than the one in Fig. 6(b). This is why the offset in Fig. 5(a) is larger when compared to Fig. 6(a).

B. Gaussian disorder in the oxidation thickness

In this section, We denote the oxidation thickness at junction as w_α and assume it is a Gaussian random variable

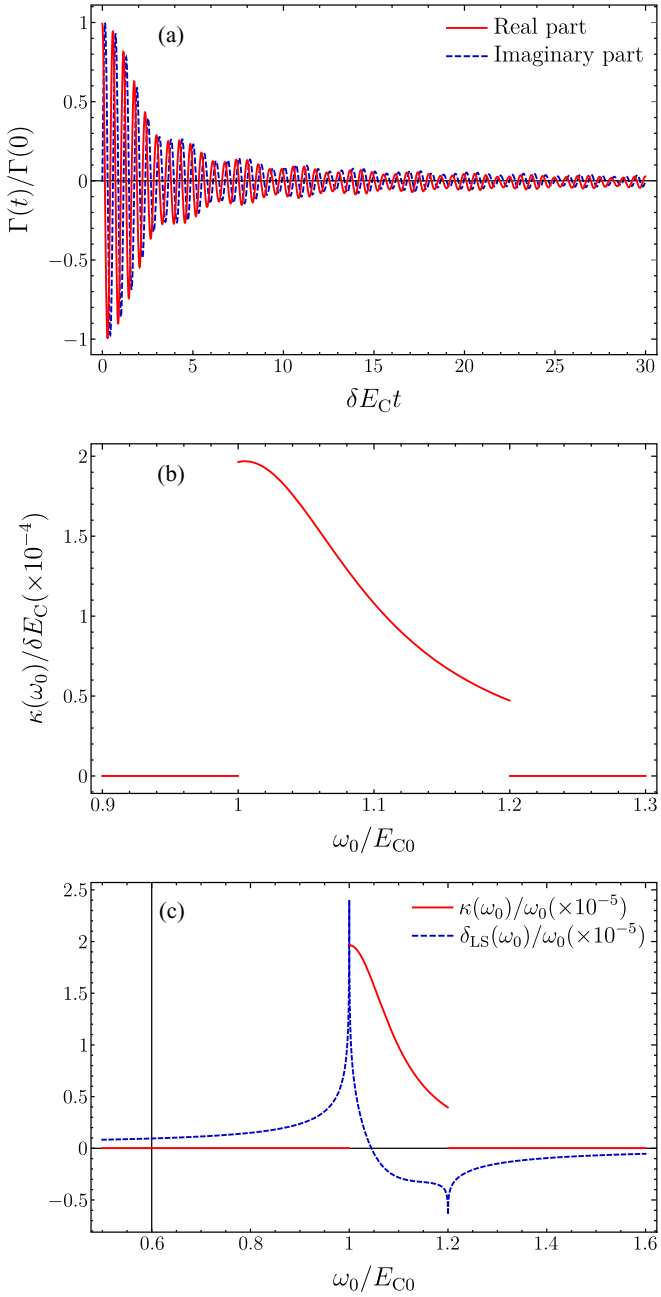

FIG. 4. (a) The normalized correlation function of the JJA, $\Gamma(t)/\mathrm{Re}[\Gamma(0)]$. (b) The decay rate versus the frequency of the LC oscillator. (c) The ratio between Lamb shift and the decay rate over the frequency of the LC oscillator. The chain is in the limit of zero-temperature given by Eq. (72), where the bath correlation function decays rapidly compared to the decay timescale of the oscillator, as shown in panels (a) and (b). Other parameters for the junction chain is the same as Fig. 3. The value for the LC oscillator and the coupling $\varepsilon_I = 0.01$, $E_Q = 100E_{C0}$, and $\delta E_C = 0.1E_{C0}$. The decay rate, proportional to the spectral density shown in Fig. 3, is nonzero only when the frequency of the LC oscillator ω_0 is resonant with the characteristic modes in the Josephson bath, whose frequencies lie in the range $[E_{C0},\ (1+a/2)E_{C0}]$. Comparing panels (a) and (b), one obviously observe that the decay of the bath correlation function is much fast than the decay of the LC oscillator so that the Born–Markov approximation is satisfied in this case. The red line in panel (c) indicates that the decay rate is much smaller than the frequency of the LC oscillator such that the secular approximation is satisfied.

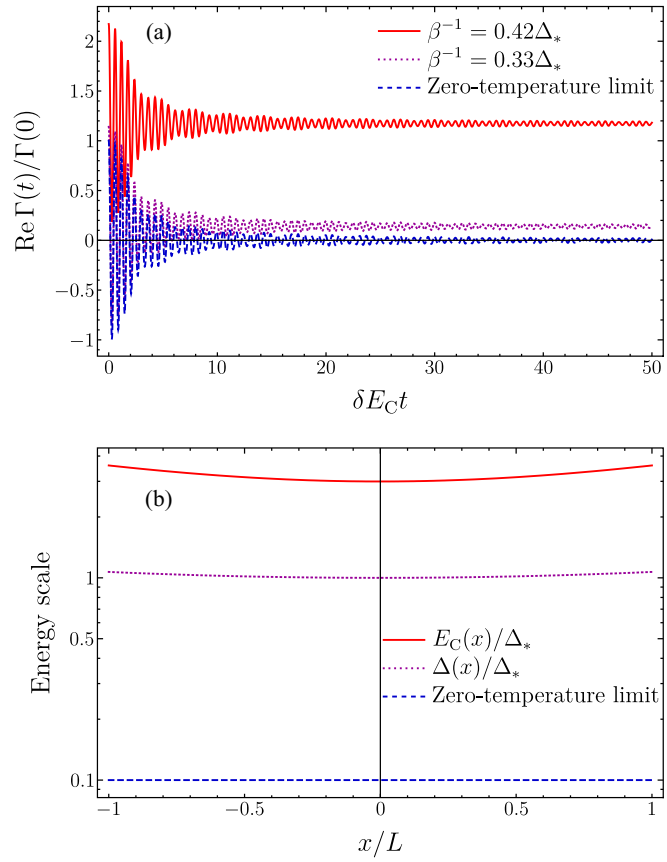

FIG. 5. (a) The real part of the normalized correlation function versus time. (b) The distribution of the energy scales of the $\Delta(x)$, $E_C(x)$ and the zero-temperature limit (given by the blue dashed lines) are $\beta^{-1} \lesssim \Delta_*/10$. The junction parameters are the same as described in the caption of Fig. 3. In particular, $E_C \in [1,\ 1.2]E_{C0}$, $E_{J0} = E_{C0}/20$, $\delta E_C = 0.1E_{C0}$, and $\Delta_* = \Delta(0) = 0.33E_{C0}$. The normalization is performed by dividing the value of the real part of correlation function in the zero-temperature limit evaluated at $t = 0$. The blue dashed line in panel (a) corresponding to the normalized correlation function in the zero-temperature limit is the same as the one shown in Fig. 4. The offset in the correlation function for $\beta^{-1} = 0.42\Delta_*$ shown in red solid line in panel (a) is about 100% when compared to the magnitude for the correlation function in the zero-temperature limit. We note that the shape of $\Delta(x)$ in panel (b) is quite flat. This indicates when the temperature is increased beyond the zero-temperature limit for $x_* = 0$, significant portion of near the origin will also violate the zero-temperature. This accounts for the huge offset in panel (a).

with mean w_0 and width δw. From Eqs. (91) and (92), we immediately

In the continuum limit, the correlation function Eq. (69) can be written as

$$\Gamma(t) = \frac{\varepsilon_I^2 N_J F_J^2 A^2}{2e^2\zeta^2}\int_{w_{\min}}^{\infty} dw\,\frac{\mathcal{P}(w)}{\sinh^2(w/\zeta)}e^{2ie^2wt/(\epsilon_r A)}. \quad (103)$$

Comparing with Eq. (70), we see that w and $N_J\mathcal{P}(w)$ play the roles of x and $v(x)$, respectively. The plots of correlation function, decay rate and Lamb shift are shown in Fig. 7. While it is clear that the JJA bath correlation time decreases with the width of the disorder δE_C, it is straightforward to show that for

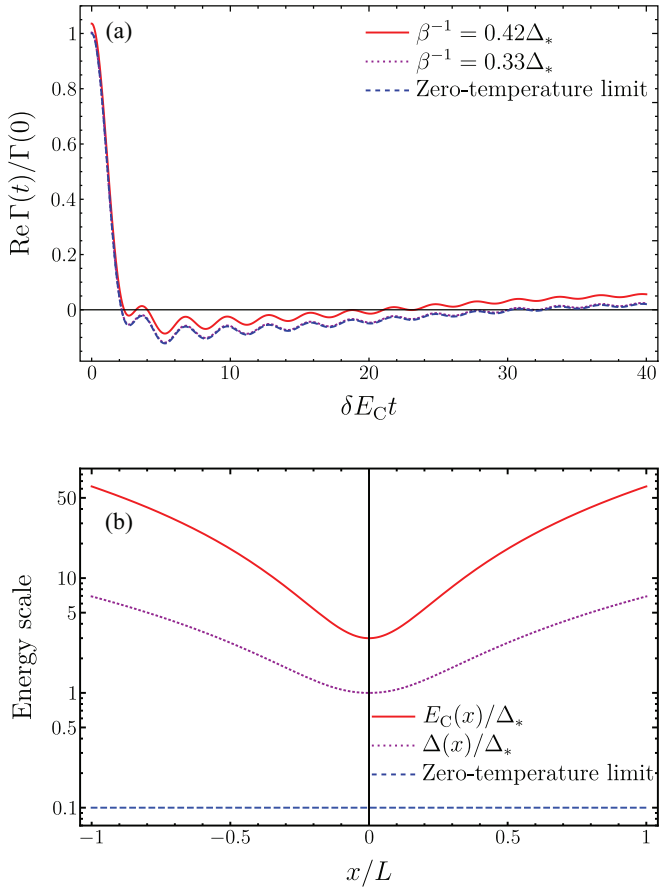

FIG. 6. (a) The real part of the normalized correlation function versus time. (b) The distribution of the energy scales of the $\Delta(x)$, $E_C(x)$ and the zero-temperature limit (given by the blue dashed lines) are $\beta^{-1} \lesssim \Delta_*/10$. The junction parameter $a = 40$ so that $E_C \in [1,\ 21]E_0$, wider than Fig. 5. Other parameters: $E_{J0} = E_{C0}/20$, $\mathcal{A} = 50$, $\sigma = 0.25$, $E_Q = 100E_{C0}$, $\varepsilon_I = 0.01$, $\delta E_C = 10E_{C0}$, and $\Delta_* = \Delta(0) = 0.33E_{C0}$. The normalization of the correlation function in panel (a) is performed by dividing the value of the real part of the correlation function in the zero-temperature limit evaluated at $t = 0$. The blue dashed line in panel (a) corresponding to the normalized correlation function in the zero-temperature limit is the same as the one shown in Fig. 4. The offset in the correlation function for $\beta^{-1} = 0.42\Delta_*$ shown in red solid line in panel (a) is about 5% when compared to the magnitude for the correlation function in the zero-temperature limit. Note that the shape of $\Delta(x)$ in panel (b) is more warped than that in Fig. 5(b). Therefore, we expect when the temperature is increased beyond the zero-temperature limit near $x_* = 0$, offset in the correlation function should be smaller than that in Fig. 5(a).

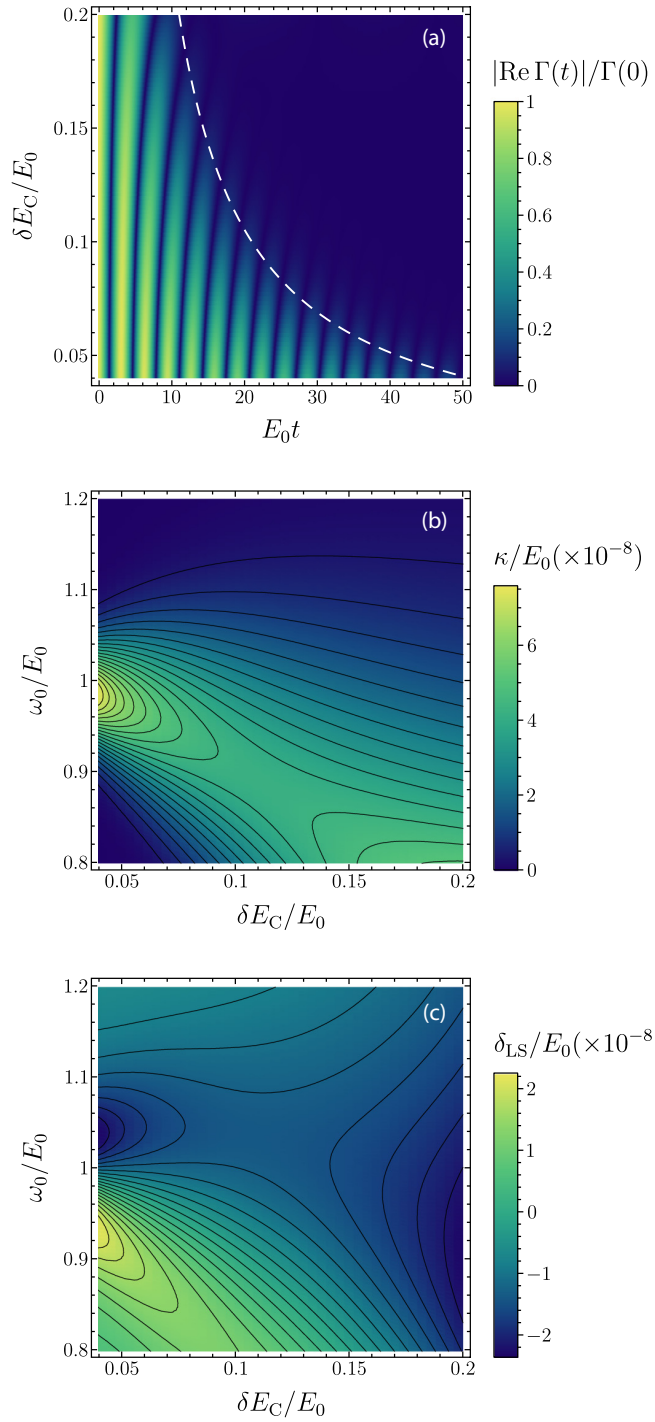

FIG. 7. 2D plots of (a) the normalized magnitude of the real part of the Josephson bath correlation function $|\mathrm{Re}\Gamma(t)|/\Gamma(0)$ versus time and the width of the disorder, (b) the normalized decay rate κ/E_0 versus the width of the disorder and the oscillator frequency, and (c) the normalized Lamb shift δ_{LS}/E_0 versus the width of the disorder and the oscillator frequency. Values of parameters: $F_J A/\zeta = E_0/100$, $E_{min} = E_\zeta = E_0/5$, $E_Q = 2E_0$, $\varepsilon_I = 0.01$, and $N_J = 10000$.

fixed oscillator frequency ω_0 and E_0, the decay rate reaches its maximum when $\delta E_C = \sqrt{2}|\omega_0 - E_0|$. Note that in Fig. 7(b), the ratio of $\kappa/\omega_B \sim \kappa/(10\delta E_C)$ is of the order 10^{-5}, similar to the atomic case where [3,4] $\kappa/\omega_B \sim 10^{-7}$–$10^{-6}$.

VII. DISCUSSION AND CONCLUSION

We showed that when the charging energy is the largest energy scale comparing to temperature and the Josephson energy, a 1D Josephson junctions array (JJA) can behave as a Markovian bath of nonlinear rotors provided the distribution for the chain parameters meet specific conditions, namely, the leading-order of the bath correlation function decays rapidly. We calculated the dynamics of an LC oscillator that is coupled

to the JJA the using approach of the GKSL Markovian master equation. In particular, we derived explicit expressions of the Lamb shift and decay rate of the LC oscillator caused by the coupling to the JJA. We found the leading order of the JJA bath correlation function in the large charging energy regime bears the same form as that of a harmonic bath, which can be approximated in the large Josephson energy regime to the leading order. Based on this observation, we established a mapping between the junction parameters in the two regimes, identifying the set of parameters inducing the same coarse-grained dynamics for a small quantum system coupled to the chain. We gave two specific examples and showed that it fits into the GKSL framework. In the first example the spatial distributions of junction density and charging energy are properly engineered such that effective spectral density is a Lorentzian while in the second example the charging energy is a Gaussian random variable so that the effective spectral density is a Gaussian.

When the temperature is increased to the point where a large region across chain is beyond the zero-temperature limit, the JJA bath correlation function gets significantly shifted by a constant, which renders the dynamics of the LC oscillator non-Markovian. This phenomenon is an indication that beyond the zero-temperature limit the primary system is correlated with the JJA bath on a very long timescale, which cannot be addressed within the framework of the GKSL master equation approach. Sophisticated techniques aiming at tackling such non-Markovian effects will be further explored in the future. Other possible future directions may include generalizing the discussion here to other types of geometry of JJA, investigating strong-coupling and strong nonlinear effects, etc.

ACKNOWLEDGMENTS

Work by J.Y., E.J., C.E., and A.N.J. was supported by the U.S. Department of Energy (DOE), Office of Science, Basic Energy Sciences (BES) under Award No. DE-SC0017890. Work by K.L.H. was funded by ANR BOCA.

APPENDIX A: DERIVATION OF THE GKSL MASTER EQUATION

In this section, we start with Eqs. (1), (4), and (5) to derive the GKSL master equation, following the standard procedure in Refs. [3] and [4]. Assuming

$$\rho_{\rm tot}(t) = \rho_{\rm S}(t) \otimes \rho_{\rm B}. \tag{A1}$$

By moving to the interaction picture associated with the free Hamiltonian Eqs. (1) and (4), we obtain the following Redfield master equation

$$\frac{d\rho_{\rm S}}{dt} = -\int_0^t dt' {\rm Tr}_{\rm B}\{H_{\rm I}(t),\ [H_{\rm I}(t'),\ \rho_{\rm S}(t)\otimes\rho_{\rm B}]\}, \tag{A2}$$

where

$$H_{\rm I}(t) \equiv e^{i(H_{\rm S}+H_{\rm B})t} H_{\rm I} e^{i(H_{\rm S}+H_{\rm B})t}. \tag{A3}$$

In Eq. (A2), we have used the fact that ${\rm Tr}_{\rm B}(H_{\rm I}\rho_{\rm B}) = 0$, which has been justified below Eq. (25) in the main text. Performing the Born–Markov approximation, we obtain

$$\begin{aligned}&\int_0^t dt' {\rm Tr}_{\rm B}\{H_{\rm I}(t),\ [H_{\rm I}(t'),\ \rho_{\rm S}(t)\otimes\rho_{\rm B}]\}\\ &= \int_0^\infty ds\,\Gamma(s)[Q(t)Q(t-s)\rho_{\rm S}(t) - Q(t)\rho_{\rm S}(t)Q(t-s)]\\ &\quad + {\rm H.c.},\end{aligned} \tag{A4}$$

where $\Gamma(s)$ is defined as Eq. (28) and

$$Q(t) \equiv e^{iH_{\rm S}t} Q e^{-iH_{\rm S}t}. \tag{A5}$$

Therefore, we find

$$Q(t) = -i\sqrt{\frac{C\omega_0}{2}}(be^{-i\omega t} - b^\dagger e^{i\omega t}). \tag{A6}$$

Substituting Eq. (A6) into the first term on the right-hand side of Eq. (A4), one obtains

$$\begin{aligned}&\int_0^\infty ds\,\Gamma(s)Q(t)Q(t-s)\rho_{\rm S}(t)\\ &= \frac{C\omega_0}{2}\int_0^\infty ds\,\Gamma(s)(be^{-i\omega_0 t} - b^\dagger e^{i\omega_0 t})\\ &\quad\times(b^\dagger e^{i\omega_0(t-s)} - be^{-i\omega_0(t-s)})\rho_{\rm S}(t)\\ &= \frac{C\omega_0}{2}[\Gamma(-\omega_0)bb^\dagger + \Gamma(\omega_0)b^\dagger b]\rho_{\rm S}(t),\end{aligned} \tag{A7}$$

where we have performed the secular approximation to drop the anti-rotating and energy nonconservation terms. Similarly, we find

$$\begin{aligned}&\int_0^\infty ds\,\Gamma(s)Q(t)\rho_{\rm S}(t)Q(t-s)\\ &= \frac{C\omega_0}{2}[\Gamma(-\omega)b\rho_{\rm S}(t)b^\dagger + \Gamma(\omega)b^\dagger\rho_{\rm S}(t)b].\end{aligned} \tag{A8}$$

Defining $\gamma(\omega_0)$ and $s(\omega_0)$ as

$$\gamma(\omega_0) = 2{\rm Re}\Gamma(\omega_0), \tag{A9}$$

$$s(\omega_0) = -{\rm Im}\Gamma(\omega_0), \tag{A10}$$

we may rewrite

$$\begin{aligned}\Gamma(-\omega_0)bb^\dagger\rho_{\rm S}(t) + {\rm H.c.} &= \tfrac{1}{2}\gamma(-\omega_0)\{\rho_{\rm S}(t),\ bb^\dagger\}\\ &\quad + {\rm i}s(-\omega_0)[bb^\dagger,\ \rho_{\rm S}(t)],\end{aligned} \tag{A11}$$

$$\begin{aligned}\Gamma(\omega_0)b^\dagger b\rho_{\rm S}(t) + {\rm H.c.} &= \tfrac{1}{2}\gamma(\omega_0)\{\rho_{\rm S}(t),\ b^\dagger b\}\\ &\quad + {\rm i}s(\omega_0)[b^\dagger b,\ \rho_{\rm S}(t)],\end{aligned} \tag{A12}$$

$$\Gamma(\omega_0)b^\dagger\rho_{\rm S}(t)b + {\rm H.c.} = \gamma(\omega_0)b^\dagger\rho_{\rm S}(t)b, \tag{A13}$$

$$\Gamma(-\omega_0)b\rho_{\rm S}(t)b^\dagger + {\rm H.c.} = \gamma(-\omega_0)b\rho_{\rm S}(t)b^\dagger. \tag{A14}$$

Substituting Eqs. (A4), (A7), (A8), (A11), and (A14) into Eq. (A2) gives

$$\begin{aligned}\frac{d\rho_{\rm S}}{dt} &= -{\rm i}[\rho_{\rm S}(t),\ H_{\rm LS}] + \kappa(\omega_0)\mathcal{D}[b]\rho_{\rm S}(t)\\ &\quad + \cancel{\kappa(-\omega_0)\mathcal{D}[b^\dagger]\rho_{\rm S}(t)},\end{aligned} \tag{A15}$$

where

$$H_{\mathrm{LS}} = \frac{C\omega_0}{2}\{[s(\omega)+s(-\omega)]b^\dagger b + s(-\omega)\}, \quad \text{(A16)}$$

$$\kappa(\omega_0) = \frac{C\omega_0}{2}\gamma(\omega_0), \quad \text{(A17)}$$

$$\mathcal{D}[A]\rho_{\mathrm{S}}(t) \equiv A^\dagger \rho_{\mathrm{S}}(t) A - \frac{1}{2}\{\rho_{\mathrm{S}}(t),\, A^\dagger A\}. \quad \text{(A18)}$$

Note that according to Eq. (83) in the main text, the spontaneous absorption rate $\kappa(-\omega_0)$ is zero. Therefore, Eq. (A15) reduces to Eq. (79) in the main text.

APPENDIX B: PERTURBATIVE EVALUATION OF THE SINGLE-JUNCTION TWO-POINT CORRELATION FUNCTION AT LOW TEMPERATURE

1. Time-independent perturbation method

We consider a single Josephson junction in the regime $E_{\mathrm{J}} \ll E_{\mathrm{C}}$. The corresponding Hamiltonian is $H = H_{\mathrm{C}} + \lambda H_{\mathrm{J}}$, with $H_{\mathrm{C}} = E_{\mathrm{C}}N^2$, $H_{\mathrm{J}} = -E_{\mathrm{C}}\cos\varphi$, and $\lambda = E_{\mathrm{J}}/E_{\mathrm{C}} \ll 1$. Since the Hamiltonian commutes with the charge conjugation operator C, we choose to work in a common eigenbasis of H and C. The states of such basis are denoted by $|\psi_{n,\pm}\rangle$, with

$$H\,|\psi_{n,\pm}\rangle = E_{n,\pm}\,|\psi_{n,\pm}\rangle\,, \quad \text{(B1)}$$

$$C\,|\psi_{n,\pm}\rangle = \pm\,|\psi_{n,\pm}\rangle\,. \quad \text{(B2)}$$

The Josephson Hamiltonian H_{J} will be treated as a perturbation, λ being assumed to be small. Applying time-independent perturbation theory [52] to lowest nonvanishing order in λ, we derive the correlation function $G(t) = \langle N(t)N(0)\rangle$, where time dependence indicates that we consider operators in the Heisenberg picture (with respect to Hamiltonian H). The average value is taken over the thermal state with inverse temperature β,

$$\rho = \frac{1}{Z}e^{-\beta H}, \quad \text{(B3)}$$

where $Z = \mathrm{Tr}e^{-\beta H}$ is the partition function. The correlation function is then expanded as follows:

$$G(t) = \frac{\mathrm{Tr}(e^{-\beta H}e^{iHt}Ne^{-iHt}N)}{\mathrm{Tr}e^{-\beta H}} = \frac{\sum_{m,n,\pm}|\langle\psi_{m,\pm}|N|\psi_{n,\mp}\rangle|^2 e^{-\beta E_{m,\pm}}e^{i(E_{m,\pm}-E_{n,\mp})t}}{\sum_{n,\pm}e^{-\beta E_{n,\pm}}}. \quad \text{(B4)}$$

In the numerator above, we have taken into account the fact that the number operator N only couples states of different charge parities.

Let us now compute the approximate eigenstates and eigenenergies of the Josephson junction Hamiltonian using time-independent perturbation theory. We consider the following expansions in powers of λ,

$$|\psi_{n,\pm}\rangle = \sum_{q=0}^{\infty}\lambda^q\,|\psi_{n,\pm}^{(q)}\rangle, \quad \text{(B5)}$$

$$E_{n,\pm} = \sum_{q=0}^{\infty}\lambda^q E_{n,\pm}^{(q)}. \quad \text{(B6)}$$

Equation (B1) then becomes

$$(H_{\mathrm{C}}+\lambda H_{\mathrm{J}})\sum_{q=0}^{\infty}\lambda^q\,|\psi_{n,\pm}^{(q)}\rangle = \left(\sum_{q=0}^{\infty}\lambda^q E_{n,\pm}^{(q)}\right)\sum_{q=0}^{\infty}\lambda^q\,|\psi_{n,\pm}^{(q)}\rangle\,. \quad \text{(B7)}$$

Sorting out the terms of same order in λ in the above equation, we obtain

$$H_{\mathrm{C}}\,|\psi_{n,\pm}^{(q)}\rangle + H_{\mathrm{J}}\,|\psi_{n,\pm}^{(q-1)}\rangle = \sum_{p=0}^{q}E_{n,\pm}^{(p)}\,|\psi_{n,\pm}^{(q-p)}\rangle\,. \quad \text{(B8)}$$

To zeroth order in λ, we simply obtain $H_{\mathrm{C}}\,|\psi_{n,\pm}^{(0)}\rangle = E_{n,\pm}^{(0)}\,|\psi_{n,\pm}^{(0)}\rangle$. This means that $E_{n,\pm}^{(0)}$ is an eigenenergy of H_{C}, so we can identify $E_{n,\pm}^{(0)} = n^2E_{\mathrm{C}}$. However, the corresponding eigenstate $|\psi_{n,\pm}^{(0)}\rangle$ cannot be fully characterized at this stage. Indeed, all energy levels except the ground state are twofold degenerate: the charge states $|n\rangle$ and $|-n\rangle$ correspond to the same eigenenergy n^2E_{C}, which means that any linear combination of these states is also an eigenstate of H_{C} with the same eigenenergy. Consequently, $|\psi_{n,\pm}^{(0)}\rangle$ can be any such combination. Here, this issue can be resolved invoking charge parity. Indeed, since the exact eigenstate $|\psi_{n,\pm}\rangle$ has a definite parity, all the corrections $|\psi_{n,\pm}^{(q)}\rangle$, in particular $|\psi_{n,\pm}^{(0)}\rangle$, must too. The only states of definite parity that can be constructed from the charge states $|n\rangle$ and $|-n\rangle$ are

$$|\chi_{n,\pm}\rangle = \frac{1}{\sqrt{2}}(|n\rangle \pm |-n\rangle). \quad \text{(B9)}$$

In conclusion, we choose $|\psi_{n,\pm}^{(0)}\rangle = |\chi_{n,\pm}\rangle$ for the excited states ($n > 0$), but we simply have $|\psi_0^{(0)}\rangle = |0\rangle$ for the ground state as it is not degenerate.

To first order in λ, Eq. (B8) yields

$$\left(H_{\mathrm{C}} - E_{n,\pm}^{(0)}\right)|\psi_{n,\pm}^{(1)}\rangle + \left(H_{\mathrm{J}} - E_{n,\pm}^{(1)}\right)|\psi_{n,\pm}^{(0)}\rangle = 0. \quad \text{(B10)}$$

We obtain the first-order energy correction by projecting this equation onto $|\psi_{n,\pm}^{(0)}\rangle$,

$$E_{n,\pm}^{(1)} = \langle\psi_{n,\pm}^{(0)}|H_{\mathrm{J}}|\psi_{n,\pm}^{(0)}\rangle. \quad \text{(B11)}$$

It is clear that $E_{n,\pm}^{(1)} = 0$, because H_{J} only couples neighboring charge states,

$$\langle m|H_{\mathrm{J}}|n\rangle = -\frac{E_{\mathrm{C}}}{2}(\delta_{m,n+1} + \delta_{m,n-1}). \quad \text{(B12)}$$

As such, the perturbation will not induce any correction to the energy to first order in λ. However, there still are corrections to the states. Indeed, projecting Eq. (B10) onto $|\psi_{m,\pm}^{(0)}\rangle$, $m \neq n$, we find

$$\langle\psi_{m,\pm}^{(0)}|\psi_{n,\pm}^{(1)}\rangle = -\frac{\langle\psi_{m,\pm}^{(0)}|H_{\mathrm{J}}|\psi_{n,\pm}^{(0)}\rangle}{E_m^{(0)} - E_n^{(0)}} = \frac{\langle\psi_{m,\pm}^{(0)}|\cos\varphi|\psi_{n,\pm}^{(0)}\rangle}{m^2 - n^2}. \quad \text{(B13)}$$

Note that, for all m, $\langle\psi_{m,\mp}^{(0)}|\psi_{n,\pm}^{(1)}\rangle = 0$ since states of different charge parities do not overlap. In particular, $\langle\psi_{n,\mp}^{(0)}|\psi_{n,\pm}^{(1)}\rangle = 0$. At this stage, only the component of $|\psi_{n,\pm}^{(1)}\rangle$ along $|\psi_{n,\pm}^{(0)}\rangle$ is still undetermined. It can be obtained invoking the normalization of the exact eigenstate, $\langle\psi_{n,\pm}|\psi_{n,\pm}\rangle = 1$. Furthermore, we set the phase of $|\psi_{n,\pm}\rangle$ by imposing $\langle\psi_{n,\pm}^{(0)}|\psi_{n,\pm}\rangle \in \mathbb{R}$. To first

order in λ, this yields $\langle\psi^{(0)}_{n,\pm}|\psi^{(1)}_{n,\pm}\rangle = 0$. We then conclude

$$|\psi^{(1)}_{n,\pm}\rangle = \sum_{m\neq n} \frac{\langle\psi^{(0)}_{m,\pm}|\cos\varphi|\psi^{(0)}_{n,\pm}\rangle}{m^2-n^2}\,|\psi^{(0)}_{m,\pm}\rangle. \tag{B14}$$

For $n = 0$, this yields

$$|\psi^{(1)}_{0}\rangle = \frac{1}{\sqrt{2}}\,|\chi_{1,+}\rangle. \tag{B15}$$

For $n = 1$, we have

$$|\psi^{(1)}_{1,+}\rangle = \frac{1}{6}\,|\chi_{2,+}\rangle + \frac{1}{\sqrt{2}}\,|0\rangle, \tag{B16}$$

$$|\psi^{(1)}_{1,-}\rangle = \frac{1}{6}\,|\chi_{2,-}\rangle. \tag{B17}$$

Finally, for $n > 1$, we find

$$|\psi^{(1)}_{n,\pm}\rangle = \frac{1}{2}\left(\frac{1}{2n+1}\,|\chi_{n+1,\pm}\rangle - \frac{1}{2n-1}\,|\chi_{n-1,\pm}\rangle\right). \tag{B18}$$

To second order in λ, Eq. (B8) yields

$$\left(H_C - E^{(0)}_{n,\pm}\right)|\psi^{(2)}_{n,\pm}\rangle + \left(H_J - E^{(1)}_{n,\pm}\right)|\psi^{(1)}_{n,\pm}\rangle = E^{(2)}_{n,\pm}\,|\psi^{(0)}_{n,\pm}\rangle. \tag{B19}$$

As before, we project this equation onto $|\psi^{(0)}_{n,\pm}\rangle$ to find

$$E^{(2)}_{n,\pm} = \langle\psi^{(0)}_{n,\pm}|H_J|\psi^{(1)}_{n,\pm}\rangle = -E_C\sum_{m\neq n}\frac{\left|\langle\psi^{(0)}_{m,\pm}|\cos\varphi|\psi^{(0)}_{n,\pm}\rangle\right|^2}{m^2-n^2}. \tag{B20}$$

For $n = 0$, this yields

$$E^{(2)}_{0} = -\frac{E_C}{2}. \tag{B21}$$

For $n = 1$, we find

$$E^{(2)}_{1,+} = \frac{5E_C}{12}, \tag{B22}$$

$$E^{(2)}_{1,-} = -\frac{E_C}{12}. \tag{B23}$$

Interestingly, the degeneracy of the first excited states is lifted here. However, this is not the case for higher-energy excited states since, for $n > 1$, we have

$$E^{(2)}_{n,\pm} = \frac{E_C}{2(4n^2-1)}. \tag{B24}$$

We can now use the results of our perturbative calculation to derive the correlation function in Eq. (B4). For simplicity, corrections to the energies will be neglected in the oscillating exponentials. This approximation is justified for short times, $t \ll 1/(\lambda^2 E_C)$. This is not an issue as the main purpose of our study is to describe the short-time dynamics of correlations. We can perform the same type of approximation for the Boltzmann factors, which corresponds to the high-temperature regime $\beta^{-1} \gg \lambda^2 E_C$. More generally, our perturbative calculation of the energies to second order in λ seems insufficient to access the long times or low temperatures, $t \gtrsim 1/(\lambda^3 E_C)$ or $\beta^{-1} \lesssim \lambda^3 E_C$.

To leading order in λ, we find that only the states $|\psi_{n,\pm}\rangle$ and $|\psi_{n,\mp}\rangle$ degenerate when $\lambda = 0$ but corresponding to different charge parities, contribute to correlations,

$$\langle\psi_{m,\pm}|N|\psi_{n,\mp}\rangle = m\delta_{mn} + O(\lambda). \tag{B25}$$

The correlation function can then be approximated by

$$G(t) \approx \frac{2\sum_{n=1}^{\infty} n^2 e^{-n^2\beta E_C}}{1+2\sum_{n=1}^{\infty} e^{-n^2\beta E_C}}. \tag{B26}$$

Actually, it is also possible to obtain the correlation function in the low-temperature regime. In this case, we neglect the contribution of excited states to the summations in Eq. (B4). In this context, the Boltzmann factors $e^{\beta E_0}$ cancel each other we do not need an accurate expression for E_0. The typical energy gap between two energy levels is the charging energy E_C—or rather E_C is a lower bound of the gap—so this approximation is typically justified when $\beta^{-1} \ll E_C$. The correlation function is then approximated by

$$G(t) \approx \sum_n |\langle\psi_0|N|\psi_{n,-}\rangle|^2 e^{-i(E_{n,-}-E_0)t}. \tag{B27}$$

To leading order in λ, only the state $|\psi_{1,-}\rangle$ contributes to the summation above, $\langle\psi_0|N|\psi_{n,-}\rangle = \lambda/\sqrt{2} + O(\lambda^2)$. As a result, we find, for $t \ll 1/(\lambda^2 E_C)$,

$$G(t) \approx \frac{\lambda^2}{2} e^{-iE_C t}. \tag{B28}$$

As the temperature is increased, we can include the contributions from excited states in the summations of Eq. (B4) to analyze the transition from Eq. (B28) to Eq. (B26). For example, when $e^{-\beta E_C} \sim \lambda^2$, it becomes relevant to take into account the contribution of the first excited states to lowest order in λ. The correlation function can then be approximated by

$$G(t) \approx \frac{\lambda^2}{2} e^{-iE_C t} + 2e^{-\beta E_C}. \tag{B29}$$

2. Matsubara formalism

The two-point correlation function for a single junction can alternatively be calculated from the Matsubara formalism [53,54]. Starting from Eqs. (42) and (43), we analytically continue to the imaginary time and obtain the Schrödinger equation in the interaction picture as

$$\partial_\tau U_I(\tau) = \lambda H_I(\tau) U_I(\tau), \tag{B30}$$

where $H_I(\tau) = -e^{\tau H_C} H_J e^{-\tau H_C}$. The imaginary time propagator $U_I(\tau)$ can be explicitly expressed as

$$U_I(\tau) = e^{\tau H_C} e^{-\tau H}, \tag{B31}$$

which can be verified by substituting into Eq. (B30). With Eqs. (B30) and (B31), we find

$$\mathrm{Tr}[e^{-\beta H}] = \mathrm{Tr}[e^{-\beta H_C} U_I(\beta)], \tag{B32}$$

$$\mathrm{Tr}[e^{-\beta H} N(\tau)] = \mathrm{Tr}[e^{-\beta H_C} U_I(\beta) N(0)], \tag{B33}$$

and

$$\begin{aligned}&\mathrm{Tr}[e^{-\beta H} N(\tau) N(0)]\\ &\quad= \mathrm{Tr}\left[e^{-\beta H_C} U_I(\beta) U_I^{-1}(\tau) N_I(\tau) U_I(\tau) N(0)\right]\\ &\quad= \mathrm{Tr}[e^{-\beta H_C}\mathcal{T}(U_I(\beta) N_I(\tau) N(0))],\end{aligned} \tag{B34}$$

where $N_I(\tau) \equiv e^{\tau H_C} N(0) e^{-\tau H_C}$ is the number operator in the interaction picture. To the second order of λ, we

find

$$U_I(\tau) = 1 + \lambda \int_0^\tau d\tau' H_I(\tau') + \lambda^2 \int_0^\tau d\tau' \int_0^{\tau'} d\tau'' H_I(\tau') H_I(\tau'') + \cdots . \quad \text{(B35)}$$

In the free rotor basis $\langle \varphi | n \rangle = e^{in\varphi}/\sqrt{2\pi}$, which are eigenstates of N and H_C with eigenvalues n and $n^2 E_C$, respectively, we find

$$\langle n | \cos\varphi | m \rangle = \frac{1}{2}(\delta_{n+1,m} + \delta_{n-1,m}), \quad \text{(B36)}$$

$$\langle n | \cos\varphi | k \rangle \langle k | \cos\varphi | m \rangle = \frac{1}{4}(\delta_{n+1,k}\delta_{k+1,m} + \delta_{n+1,k}\delta_{k-1,m} + \delta_{n-1,k}\delta_{k+1,m} + \delta_{n-1,k}\delta_{k-1,m}). \quad \text{(B37)}$$

Therefore,

$$\langle n | H_I(\tau') | n \rangle = 0, \quad \text{(B38)}$$

$$\langle n | H_I(\tau') | k \rangle \langle k | H_I(\tau'') | n \rangle = \frac{E_C^2}{4}[\delta_{n+1,k} F_n(\tau' - \tau'') + \delta_{n-1,k} F_{-n}(\tau' - \tau'')], \quad \text{(B39)}$$

where

$$F_n(\tau) = \exp[-E_C \tau (1 + 2n)]. \quad \text{(B40)}$$

Equation (B32) can be rewritten as

$$\mathrm{Tr}[e^{-\beta H}] = \sum_n e^{-\beta E_C n^2} \langle n | U_I(\beta) | n \rangle . \quad \text{(B41)}$$

To the second order of λ, according to Eqs. (B35), (B38), and (B39), we find

$$\langle n | U_I(\beta) | n \rangle = 1 - \frac{\lambda^2 E_C^2}{4}[K_n(\beta) + K_{-n}(\beta)] + O(\lambda^3), \quad \text{(B42)}$$

where

$$K_n(\tau) = \int_0^\tau d\tau' \int_0^{\tau'} d\tau'' F_n(\tau' - \tau'') = \frac{1}{(1+2n)^2 E_C^2} e^{-\tau E_C (1+2n)} + \frac{\tau}{(1+2n) E_C} - \frac{1}{(1+2n)^2 E_C^2}. \quad \text{(B43)}$$

The infinite series in the right-hand side of Eq. (B41) can be evaluated at the limit $\beta E_C \gg 1$, where the infinite sum is replaced by the lowest order in $e^{-\beta E_C}$ in the summand. Therefore,

$$\sum_n e^{-\beta E_C n^2} K_n(\beta) = \sum_n e^{-\beta E_C n^2} K_{-n}(\beta) = \sum_n \frac{1}{(1+2n)^2 E_C^2} e^{-\beta E_C (n+1)^2} + \sum_n \left[\frac{\beta}{(1+2n) E_C} - \frac{1}{(1+2n)^2 E_C^2} \right] e^{-\beta E_C n^2} = \frac{\beta}{E_C}. \quad \text{(B44)}$$

Therefore, we find

$$\mathrm{Tr}[e^{-\beta H}] = 1 - \frac{\beta E_C \lambda^2}{2} + O(\lambda^2) O(e^{-\beta E_C}). \quad \text{(B45)}$$

According to Eq. (B42), we observe that $\langle n | U_I(\beta) | n \rangle$ is even in n up the second order in λ. Therefore, we find

$$\mathrm{Tr}[e^{-\beta H_C} U_I(\beta) N(0)] = \sum_n n e^{-n^2 \beta E_C} \langle n | U_I(\beta) | n \rangle = O(\lambda^3) \quad \text{(B46)}$$

to all orders of $e^{-\beta E_C}$. To evaluate Eq. (B34), let us first calculate the following:

$$\langle n | \mathcal{T}(U_I(\beta) N_I(\tau) N(0)) | n \rangle = \langle n | N_I(\tau) N(0) | n \rangle + \lambda \int_0^\beta d\tau' \langle n | \mathcal{T}(H_I(\tau') N_I(\tau) Q(0)) | n \rangle + \frac{\lambda^2}{2} \int_0^\beta d\tau' \int_0^\beta d\tau'' \langle n | \mathcal{T}(H_I(\tau') H_I(\tau'') N_I(\tau) Q(0)) | n \rangle + O(\lambda^3), \quad \text{(B47)}$$

where the second term in the right-hand side vanish is due to Eq. (B38). Now let us evaluate the last term in the right-hand side of Eq. (B47). It can be written as four parts $\lambda^2/2 \sum_{k=1}^4 I_{kn}(\tau)$, where

$$I_{1n}(\tau) = \int_0^\tau d\tau' \int_0^\tau d\tau'' \langle n | N_I(\tau) \mathcal{T}(H_I(\tau') H_I(\tau'')) N(0) | n \rangle , \quad \text{(B48)}$$

$$I_{2n}(\tau) = \int_0^\tau d\tau' \int_\tau^\beta d\tau'' \langle n | H_I(\tau'') N_I(\tau) H_I(\tau') N(0) | n \rangle , \quad \text{(B49)}$$

$$I_{3n}(\tau) = \int_\tau^\beta d\tau' \int_0^\tau d\tau'' \langle n | H_I(\tau') N_I(\tau) H_I(\tau'') N(0) | n \rangle , \quad \text{(B50)}$$

$$I_{4n}(\tau) = \int_\tau^\beta d\tau' \int_\tau^\beta d\tau'' \langle n | \mathcal{T}(H_I(\tau') H_I(\tau'')) N_I(\tau) N(0) | n \rangle . \quad \text{(B51)}$$

Using the short-hand notation introduced in Eqs. (B40) and (B57), we find

$$I_{1n}(\tau) = \frac{E_C^2}{2}[n^2 K_n(\tau) + n^2 K_{-n}(\tau)], \quad \text{(B52)}$$

$$I_{2n}(\tau) = \frac{E_C^2}{4}[n(n+1) L_n(\tau) + n(n-1) L_{-n}(\tau)], \quad \text{(B53)}$$

$$I_{3n}(\tau) = I_{2n}(\tau), \quad \text{(B54)}$$

$$I_{4n}(\tau) = \frac{E_C^2}{2}[n^2 K_n(\beta - \tau) + n^2 K_{-n}(\beta - \tau)], \quad \text{(B55)}$$

where

$$L_n(\tau) = \int_0^\tau d\tau' \int_\tau^\beta d\tau'' F_n(\tau''-\tau') = \int_\tau^\beta d\tau' \int_0^\tau d\tau'' F_n(\tau'-\tau'') = \frac{1}{(1+2n)^2 E_C^2}\{e^{-\beta E_C(1+2n)}(1-e^{\tau E_C(1+2n)}) - e^{-\tau E_C(1+2n)} + 1\}, \quad \text{(B56)}$$

and we have used the fact that

$$\int_\tau^\beta d\tau' \int_\tau^{\tau'} d\tau'' F_n(\tau'-\tau'') = \int_0^{\beta-\tau} d\tau' \int_0^{\tau'} d\tau'' F_n(\tau'-\tau'') = K_n(\beta-\tau). \quad \text{(B57)}$$

The real-time correlation function is

$$G(t) = \frac{1}{\mathrm{Tr}(e^{-\beta H})} \sum_n e^{-\beta E_C n^2} \left(n^2 + \frac{\lambda^2}{2} \sum_{k=1}^4 I_{kn}(it) \right). \quad \text{(B58)}$$

Let us go back to the real time by replacing $\tau \to it$ in Eq. (B58) and then perform the low temperature approximation $e^{-\beta E_C} \ll 1$. We need to evaluate

$$\sum_n n^2 K_n(it) e^{-n^2 \beta E_C} = \sum_n n^2 K_{-n}(it) e^{-n^2 \beta E_C} = O(e^{-\beta E_C}), \quad \text{(B59)}$$

$$\sum_n n(n+1) L_n(it) e^{-\beta E_C n^2} = O(e^{-\beta E_C}), \quad \text{(B60)}$$

$$\sum_n n(n-1) L_{-n}(it) e^{-\beta E_C n^2} = O(e^{-\beta E_C}), \quad \text{(B61)}$$

$$\sum_n n^2 K_n(\beta - it) e^{-\beta E_C n^2} = \sum_n n^2 K_{-n}(\beta - it) e^{-\beta E_C n^2} = \frac{1}{E_C^2} e^{-iE_C t} + O(e^{-\beta E_C}). \quad \text{(B62)}$$

Based on these results, one readily observe that the leading order contributions to the Green's function are of the order $O(e^{-\beta E_C})O(\lambda^0)$ and $O([e^{-\beta E_C}]^0)O(\lambda^2)$. There first contribution comes from the first term in Eq. (B58) while the second contribution comes from $I_{4n}(it)$. Therefore, we find

$$G(t) = \frac{2e^{-\beta E_C} + \lambda^2 e^{-iE_C t}/2 + O(\lambda^2)O(e^{-\beta E_C})}{1 - \beta E_C \lambda^2/2 + O(\lambda^2)O(e^{-\beta E_C})}. \quad \text{(B63)}$$

From the numerator of Eq. (B63), one concludes that as long as $e^{-\beta E_C}$, $\lambda \ll 1$, the numerator is a good approximation to $\mathrm{Tr}[N_I(t)N(0)e^{-\beta H}]$. From the denominator of see that the Matsubara perturbative approach works well if $\beta E_C \lambda^2 \ll 1$. Keeping only second order of λ^2 and the first order in $e^{-\beta E_C}$, one can replace the denominator in Eq. (B63) with 1 and obtain Eq. (68). Furthermore, in the zero-temperature limit given by Eq. (40), $e^{-\beta E_C} \ll \lambda^2$ and therefore Eq. (B63) reduces to Eq. (41) in the main text.

[1] V. Gorini, A. Kossakowski, and E. C. G. Sudarshan, J. Math. Phys. **17**, 821 (1976).
[2] G. Lindblad, Commun. Math. Phys. **48**, 119 (1976).
[3] C. Cohen-Tannoudji, J. Dupont-Roc, and G. Grynberg, *Atom-photon Interactions: Basic Processes and Applications* (Wiley, Hoboken, NJ, 1998), Chap. 4.
[4] H.-P. Breuer and F. Petruccione, *The Theory of Open Quantum Systems* (Oxford University Press, Oxford, 2007).
[5] L. Diósi, N. Gisin, and W. T. Strunz, Phys. Rev. A **58**, 1699 (1998).
[6] J. T. Stockburger and C. H. Mak, J. Chem. Phys. **110**, 4983 (1999).
[7] J. T. Stockburger and H. Grabert, Phys. Rev. Lett. **88**, 170407 (2002).
[8] P. P. Orth, A. Imambekov, and K. Le Hur, Phys. Rev. B **87**, 014305 (2013).
[9] K. Le Hur, L. Henriet, L. Herviou, K. Plekhanov, A. Petrescu, T. Goren, M. Schiro, C. Mora, and P. P. Orth, C. R. Phys.Quant. Simul./Simul. Quant.**19**, 451 (2018).
[10] C. Gardiner and P. Zoller, *Quantum Noise: A Handbook of Markovian and Non-Markovian Quantum Stochastic Methods with Applications to Quantum Optics*, 3rd ed., Springer Series in Synergetics (Springer-Verlag, Berlin, 2004).
[11] R. P. Feynman and F. L. Vernon, Ann. Phys. **281**, 547 (1963).
[12] A. O. Caldeira and A. J. Leggett, Physica A **121**, 587 (1983).
[13] A. J. Leggett, S. Chakravarty, A. T. Dorsey, M. P. A. Fisher, A. Garg, and W. Zwerger, Rev. Mod. Phys. **59**, 1 (1987).
[14] A. J. Leggett, S. Chakravarty, A. T. Dorsey, M. P. A. Fisher, A. Garg, and W. Zwerger, Rev. Mod. Phys. **67**, 725 (1995).
[15] U. Weiss, *Quantum Dissipative Systems*, 4th ed. (World Scientific Publishing Company, River Edge, NJ, 2012).
[16] J. Schwinger, J. Math. Phys. **2**, 407 (1961).
[17] L. V. Keldysh, Sov. Phys. JETP **20**, 1018 (1965).
[18] L. P. Kadanoff, *Quantum Statistical Mechanics* (Westview Press, Cambridge, MA, 1994).
[19] I. de Vega and D. Alonso, Rev. Mod. Phys. **89**, 015001 (2017).
[20] N. Makri, J. Phys. Chem. B **103**, 2823 (1999).
[21] B. L. Hu, J. P. Paz, and Y. Zhang, Phys. Rev. D **47**, 1576 (1993).
[22] A. Blais, A. L. Grimsmo, S. M. Girvin, and A. Wallraff, arXiv:2005.12667.
[23] S. V. Panyukov and A. D. Zaikin, Phys. B: Condens. Matter **152**, 162 (1988).
[24] T. Niemczyk, F. Deppe, H. Huebl, E. P. Menzel, F. Hocke, M. J. Schwarz, J. J. Garcia-Ripoll, D. Zueco, T. Hümmer, E. Solano, A. Marx, and R. Gross, Nat. Phys. **6**, 772 (2010).
[25] J. Bourassa, F. Beaudoin, J. M. Gambetta, and A. Blais, Phys. Rev. A **86**, 013814 (2012).
[26] S. E. Nigg, H. Paik, B. Vlastakis, G. Kirchmair, S. Shankar, L. Frunzio, M. H. Devoret, R. J. Schoelkopf, and S. M. Girvin, Phys. Rev. Lett. **108**, 240502 (2012).
[27] K. Le Hur, Phys. Rev. B **85**, 140506(R) (2012).
[28] C. K. Lee, J. Cao, and J. Gong, Phys. Rev. E **86**, 021109 (2012).

[29] J. M. Moix, Y. Zhao, and J. Cao, Phys. Rev. B **85**, 115412 (2012).
[30] B. Peropadre, D. Zueco, D. Porras, and J. J. García-Ripoll, Phys. Rev. Lett. **111**, 243602 (2013).
[31] M. Goldstein, M. H. Devoret, M. Houzet, and L. I. Glazman, Phys. Rev. Lett. **110**, 017002 (2013).
[32] T. Weißl, B. Küng, E. Dumur, A. K. Feofanov, I. Matei, C. Naud, O. Buisson, F. W. J. Hekking, and W. Guichard, Phys. Rev. B **92**, 104508 (2015).
[33] P. Forn-Díaz, J. J. García-Ripoll, B. Peropadre, J.-L. Orgiazzi, M. A. Yurtalan, R. Belyansky, C. M. Wilson, and A. Lupascu, Nat. Phys. **13**, 39 (2017).
[34] F. Yoshihara, T. Fuse, S. Ashhab, K. Kakuyanagi, S. Saito, and K. Semba, Nat. Phys. **13**, 44 (2017).
[35] S. J. Bosman, M. F. Gely, V. Singh, A. Bruno, D. Bothner, and G. A. Steele, npj Quantum Inf. **3**, 46 (2017).
[36] L. Magazzù, P. Forn-Díaz, R. Belyansky, J.-L. Orgiazzi, M. A. Yurtalan, M. R. Otto, A. Lupascu, C. M. Wilson, and M. Grifoni, Nat. Commun. **9**, 1403 (2018).
[37] S. Léger, J. Puertas-Martínez, K. Bharadwaj, R. Dassonneville, J. Delaforce, F. Foroughi, V. Milchakov, L. Planat, O. Buisson, C. Naud, W. Hasch-Guichard, S. Florens, I. Snyman, and N. Roch, Nat. Commun. **10**, 5259 (2019).
[38] J. P. Martínez, S. Léger, N. Gheeraert, R. Dassonneville, L. Planat, F. Foroughi, Y. Krupko, O. Buisson, C. Naud, W. Hasch-Guichard, S. Florens, I. Snyman, and N. Roch, npj Quantum Inf. **5**, 19 (2019).
[39] P. Forn-Díaz, L. Lamata, E. Rico, J. Kono, and E. Solano, Rev. Mod. Phys. **91**, 025005 (2019).
[40] F. Yoshihara, T. Fuse, Z. Ao, S. Ashhab, K. Kakuyanagi, S. Saito, T. Aoki, K. Koshino, and K. Semba, Phys. Rev. Lett. **120**, 183601 (2018).
[41] É. Jussiau, M. Hasegawa, and R. S. Whitney, Phys. Rev. B **100**, 115411 (2019).
[42] É. Jussiau and R. S. Whitney, Europhys. Lett. **129**, 47001 (2020).
[43] K. W. Murch, U. Vool, D. Zhou, S. J. Weber, S. M. Girvin, and I. Siddiqi, Phys. Rev. Lett. **109**, 183602 (2012).
[44] N. Prokof'ev and P. Stamp, Rep. Prog. Phys. **63**, 669 (2000).
[45] R. Kuzmin, R. Mencia, N. Grabon, N. Mehta, Y.-H. Lin, and V. E. Manucharyan, Nat. Phys. **15**, 930 (2019).
[46] J.-T. Hsiang and B.-L. Hu, Phys. Rev. D **101**, 125002 (2020).
[47] J. Yang, J.-T. Hsiang, A. N. Jordan, and B. Hu, Ann. Phys. **421**, 168289 (2020).
[48] L. I. Glazman and A. I. Larkin, Phys. Rev. Lett. **79**, 3736 (1997).
[49] M. Houzet and L. I. Glazman, Phys. Rev. Lett. **122**, 237701 (2019).
[50] U. Vool and M. H. Devoret, Int. J. Circuit Theory Appl. **45**, 897 (2017).
[51] If it is not the case, then one can always redefine the system and coupling Hamiltonians H_S and H_I such that Eq. (25) holds; see Refs. [3] and [4] for more details.
[52] C. Cohen-Tannoudji, B. Diu, and F. Laloë, *Quantum Mechanics*, 2nd ed., Vol. 2 (Wiley, Hoboken, NJ, 2020), Chap. 11.
[53] A. Das, *Finite Temperature Field Theory* (World Scientific, Singapore/River Edge, NJ, 1997).
[54] G. D. Mahan, *Many-particle physics* (Springer Science & Business Media, Berlin, 2013).
[55] T. P. Orlando and K. A. Delin, *Foundations of Applied Superconductivity*, Vol. 8 (Addison-Wesley, Reading, MA, 1991).